

Platonic Hypermaps

Antonio J. Breda d'Azevedo¹ Gareth A. Jones

*Departamento de Matemática, Universidade de Aveiro
3800 Aveiro, Portugal*

*Department of Mathematics, University of Southampton
Southampton SO17 1BJ, United Kingdom*

Abstract. We classify the regular hypermaps (orientable or non-orientable) whose full automorphism group is isomorphic to the symmetry group of a Platonic solid. There are 185 of them, of which 93 are maps. We also classify the regular hypermaps with automorphism group A_5 : there are 19 of these, all non-orientable, and 9 of them are maps. These hypermaps are constructed as combinatorial and topological objects, many of them arising as coverings of Platonic solids and Kepler-Poinsot polyhedra (viewed as hypermaps), or their associates. We conclude by showing that any rotary Platonic hypermap is regular, so there are no chiral Platonic hypermaps.

1. Introduction

The convex polyhedra in \mathbf{R}^3 with the most interesting symmetry properties are the Platonic solids: these are the tetrahedron \mathcal{T} , the cube \mathcal{C} , the octahedron \mathcal{O} , the dodecahedron \mathcal{D} , and the icosahedron \mathcal{I} , described in Plato's dialogue *Timaeos* [25]. The rotation groups of \mathcal{T} , of \mathcal{C} and \mathcal{O} , and of \mathcal{D} and \mathcal{I} are isomorphic to the alternating and symmetric groups A_4 , S_4 and A_5 ; these are subgroups of index 2 in the isometry groups of these solids, isomorphic to S_4 , $S_4 \times C_2$ and $A_5 \times C_2$.

Each Platonic solid \mathcal{P} can be regarded as a map, that is, as a graph imbedded in a surface (in this case the sphere); more generally, \mathcal{P} can be regarded as a hypermap (a hypergraph imbedded in a surface), and within either category \mathcal{P} is a regular object, in Vince's sense

¹The author is grateful to the Research and Development Joint Research Centre of the Commission of the European Communities for financially supporting this research.

[27] that the automorphism group $\text{Aut } \mathcal{P}$ acts transitively on the “blades” out of which \mathcal{P} is constructed.

Our aim in this paper is to classify the *regular Platonic hypermaps*, the regular hypermaps \mathcal{H} (orientable or non-orientable) whose automorphism group $\text{Aut } \mathcal{H}$ is isomorphic to the automorphism group $G = \text{Aut } \mathcal{P} \cong S_4, S_4 \times C_2$ or $A_5 \times C_2$ of some Platonic solid \mathcal{P} ; for technical reasons in dealing with $A_5 \times C_2$ it is also useful for us to include the case $G \cong A_5$. The number of G -hypermaps (regular hypermaps \mathcal{H} with $\text{Aut } \mathcal{H} \cong G$) for each of these four groups G is given in Table 1, which also indicates how many of these hypermaps \mathcal{H} are orientable, are maps, and are orientable maps; the final column shows where we have provided more detailed information about the individual hypermaps.

G	G -hypermaps	orientable	maps	orientable maps	
S_4	13	4	9	3	§4.2
$S_4 \times C_2$	39	21	27	15	§7.2
A_5	19	0	9	0	§5.2
$A_5 \times C_2$	133	19	63	9	§6.2

Table 1. Number of G -hypermaps

In the orientable cases, we find that besides the hypermaps of genus 0 corresponding to the Platonic solids themselves, there are examples of genera 1, 3, 4, 5, 9 and 13; in the non-orientable cases the possible genera are 1, 4, 5, 6, 10, 14, 16, 20, 26, 30, 34 and 38.

The first step in the argument (which can, in principle, be applied to any finite group G) is to determine the algebraic G -hypermaps \mathcal{H} for each G ; as explained in [4], the isomorphism classes of these correspond bijectively to the orbits of $\text{Aut } G$ on the triples r_0, r_1, r_2 of involutions generating G , or equivalently to the normal subgroups H in the free product $\Delta = C_2 * C_2 * C_2$ with $\Delta/H \cong G$. Next, the orders l_i of the products $r_j r_k$ ($\{i, j, k\} = \{0, 1, 2\}$) in G give us the type (l_0, l_1, l_2) of each \mathcal{H} , and from this we can calculate its Euler characteristic; \mathcal{H} is orientable if and only if H lies in the “even subgroup” Δ^+ of index 2 in Δ , and knowing this we can then calculate the genus of \mathcal{H} . (This rather brief outline ignores certain questions involving boundary components, since they do not exist for our chosen groups G .)

The final stage in the process is to use this information to construct the G -hypermaps \mathcal{H} as combinatorial or topological objects. We shall do this using several techniques, including the operations on hypermaps of Machì [21] and James [16], Walsh’s correspondence [28] between hypermaps and bipartite maps, and the double coverings of hypermaps introduced in [4]. These ideas are explained in general in §2, and are described in greater detail in [4].

In §3 we introduce the Platonic solids \mathcal{P} as hypermaps, and describe their automorphism groups and rotation groups; we also describe the great dodecahedron \mathcal{GD} , a regular map of type $\{5, 5\}$ which forms the basis for several later constructions. Having described our methods in general in §2, we apply them in §§4–7 in the cases $G \cong S_4, A_5, A_5 \times C_2$ and $S_4 \times C_2$ respectively. In each of these sections we first enumerate, then describe, and finally construct the relevant hypermaps, with tables summarising their basic properties. Many of them turn out to be (or to be closely related to) such familiar objects as the regular polyhedra described by Coxeter in [8], or the regular maps described by Coxeter and Moser in [10] and classified (for low genus) by Brahana [1], Sherk [23] and Garbe [12].

Our methods of enumeration are by inspection, depending heavily on specific properties of Δ (generation by involutions) and G (faithful permutation representation of low degree, direct product decomposition, etc.). However, there are situations where one needs to vary Δ , as in §9, for instance, or G , as in [18, 19] where G is a Ree group or a Suzuki group. In such cases, direct methods may not be feasible, so in §8 we introduce a much more general enumerative method due to P.Hall [13], which in particular provides a useful numerical check for our direct calculations.

We conclude, in §9, by considering the *rotary Platonic hypermaps*. An orientable hypermap \mathcal{H} without boundary is *rotary* if its rotation group (orientation-preserving automorphism group) $\text{Aut}^+\mathcal{H}$ acts transitively on the “brins” of \mathcal{H} . (Traditionally, such hypermaps have often been called *regular* [6, 7], but we have used Wilson’s term *rotary* [30] to avoid confusion with Vince’s concept of regularity [27] used here; similarly, our regular hypermaps are termed *reflexible* in [6, 7].) Among the orientable hypermaps without boundary, “regular” implies “rotary”, but the converse is false; nevertheless we will show, using results from §8, that if \mathcal{H} is rotary with $\text{Aut}^+\mathcal{H} \cong \text{Aut}^+\mathcal{P}$ for some Platonic solid \mathcal{P} , then \mathcal{H} is regular and $\text{Aut}\mathcal{H} \cong \text{Aut}\mathcal{P}$ (so \mathcal{H} is one of the regular Platonic hypermaps classified in §§4, 6 or 7).

2. Classifying regular hypermaps

First, we briefly review the theory of regular hypermaps; see [4] or [15] for a more general account of hypermaps, and [6] for the orientable case.

If G is any group then a regular hypermap \mathcal{H} with $\text{Aut}\mathcal{H} \cong G$ is called a *regular G -hypermap*. As explained in §2 of [4], \mathcal{H} corresponds to a generating triple r_0, r_1, r_2 of G satisfying $r_i^2 = 1$ ($i = 0, 1, 2$), or equivalently to an epimorphism $\theta : \Delta \rightarrow G$, $R_i \mapsto r_i$, where Δ is the free product

$$\Delta = \langle R_0, R_1, R_2 \mid R_i^2 = 1 \rangle \cong C_2 * C_2 * C_2;$$

we call the triple $\mathbf{r} = (r_0, r_1, r_2)$ a Δ -basis for G . The set Ω of blades of \mathcal{H} can be identified with G , so that G permutes the blades by right-multiplication; the i -faces of \mathcal{H} ($i = 0, 1, 2$), that is, the hypervertices, hyperedges and hyperfaces of \mathcal{H} , are identified with the cosets gD ($g \in G$) of the dihedral subgroups $D = \langle r_1, r_2 \rangle, \langle r_2, r_0 \rangle, \langle r_0, r_1 \rangle$ of G , with incidence given by non-empty intersection. The edge-labelled trivalent graph \mathcal{G} associated with \mathcal{H} is the Cayley graph for G with respect to the Δ -basis \mathbf{r} .

The automorphisms of \mathcal{H} (or equivalently of the edge-labelled graph \mathcal{G}) are induced by the left-translations $g \mapsto x^{-1}g$ where $x \in G$, so $\text{Aut}\mathcal{H} \cong \text{Aut}\mathcal{G} \cong G$. Two regular G -hypermaps \mathcal{H} and \mathcal{H}' are isomorphic if and only if their corresponding edge-labelled graphs \mathcal{G} and \mathcal{G}' are isomorphic, that is, if and only if their Δ -bases \mathbf{r} and \mathbf{r}' are equivalent under $\text{Aut}G$. One can therefore classify the regular G -hypermaps by finding the orbits of $\text{Aut}G$ on the Δ -bases of G .

Machi’s group $S \cong S_3$ of hypermap operations [4, 21] transforms one regular G -hypermap \mathcal{H} to another (called an *associate* \mathcal{H}^π of \mathcal{H}) by renaming hypervertices, hyperedges and hyperfaces of \mathcal{H} , that is, by applying a permutation $\pi \in S_3$ to the edge-labels $i = 0, 1, 2$ of \mathcal{G} , or equivalently to the generators r_i of G . Since \mathcal{H} and \mathcal{H}^π differ only in their labelling, it is sufficient for us to find one representative from each S -orbit on the regular G -hypermaps.

Being regular, \mathcal{H} is without boundary if and only if each $r_i \neq 1$, a condition always satisfied in our case since none of our groups G can be generated by fewer than three involutions. Having empty boundary, \mathcal{H} is orientable if and only if its hypermap subgroup $H = \ker \theta$ is contained in the even subgroup $\Delta^+ = \langle R_j R_k (j \neq k) \rangle$ of index 2 in Δ ; this is equivalent to G having a subgroup G^+ of index 2 containing none of the generators r_i , in which case $G^+ \cong \Delta^+/H \cong \text{Aut}^+ \mathcal{H}$. The *type* of \mathcal{H} is (l_0, l_1, l_2) , where l_i is the order of $r_j r_k$ and $\{i, j, k\} = \{0, 1, 2\}$; thus each i -face is a $2l_i$ -gon, with sides alternately labelled j and k . There are $N_i = |G|/2l_i$ i -faces; since \mathcal{G} has $|G|$ vertices and $3|G|/2$ edges, \mathcal{H} has Euler characteristic $\chi = \sum N_i - \frac{1}{2}|G| = \frac{1}{2}|G|(\sum l_i^{-1} - 1)$. The genus of \mathcal{H} is then $g = \eta(2 - \chi)$, where $\eta = \frac{1}{2}$ or 1 as \mathcal{H} is orientable or not.

These arguments enable us to give topological descriptions of the regular G -hypermaps, and the final task is to construct them as combinatorial objects. Here we will rely on the techniques described in [4], constructing each \mathcal{H} out of some Platonic solid \mathcal{P} (with $\text{Aut } \mathcal{P} \cong G$) in such a symmetric way that each automorphism of \mathcal{P} induces an automorphism of \mathcal{H} ; thus $\text{Aut } \mathcal{H} \geq \text{Aut } \mathcal{P} \cong G$, and by comparing orders we can prove equality.

A particularly useful technique, described in greater detail in §§1 and 6 of [4], is to take a regular G -map \mathcal{M} of type $\{m, n\}$, that is, a regular G -hypermap of type $(n, 2, m)$. If \mathcal{M} is not bipartite then it does not cover the hypermap \mathcal{B}^0 (defined in §2 of [4]) which has two blades, transposed by R_0 and fixed by R_1 and R_2 ; we can therefore form the disjoint product [4, §3] $\mathcal{M}^0 = \mathcal{M} \times \mathcal{B}^0$, a regular map of type $\{m', n\}$ where $m' = \text{lcm}(m, 2)$. This is a bipartite double covering of \mathcal{M} , unbranched if m is even, and branched at the $N_2 = |G|/2m$ face-centres of \mathcal{M} if m is odd, so $\chi(\mathcal{M}^0) = 2\chi(\mathcal{M})$ or $2\chi(\mathcal{M}) - N_2$ respectively; if \mathcal{M} is orientable then so is \mathcal{M}^0 (but not conversely). Being bipartite, \mathcal{M}^0 is the Walsh map $W(\mathcal{H})$ [4, §6; 28] of a hypermap $\mathcal{H} = W^{-1}(\mathcal{M}^0)$ on the same surface as \mathcal{M}^0 : the hyperfaces of \mathcal{H} correspond to the faces of \mathcal{M}^0 , while the hypervertices and hyperedges correspond to the two monochrome sets of vertices of \mathcal{M}^0 , one vertex of each colour covering each vertex of \mathcal{M} . Thus \mathcal{H} has type (n, n, m'') , where $m'' = \frac{1}{2}m' = \frac{1}{2}m$ or m as m is even or odd. Moreover, \mathcal{H} is regular, with $\text{Aut } \mathcal{H} \cong \text{Aut } \mathcal{M} \cong G$. Many regular G -hypermaps arise in this way.

We will apply the above process to our chosen groups G , in each case enumerating, describing and finally constructing the regular G -hypermaps \mathcal{H} . In the cases $G = S_4$ and A_5 it is convenient to regard elements of G as permutations in the natural representation of degree $n = 4$ or 5 on $\{1, \dots, n\}$. In particular we will represent each involution r_i in \mathbf{r} as a disjoint set of edges (corresponding to the 2-cycles of r_i) in an n -vertex graph $\bar{\mathcal{G}}$: this is the permutation graph for G on $\{1, \dots, n\}$, or equivalently the Schreier coset graph for a point-stabiliser G_α of index n in G , with respect to a Δ -basis \mathbf{r} for G ; thus $\bar{\mathcal{G}}$ is the quotient \mathcal{G}/G_α of the Cayley graph \mathcal{G} of G corresponding to \mathbf{r} , factored out by the action of G_α on \mathcal{G} .

3. The Platonic solids as hypermaps

The Platonic solids \mathcal{P} , or more precisely their 2-skeletons, are all examples of maps (and hence hypermaps) on surfaces homeomorphic to the sphere.

The properties of the tetrahedron \mathcal{T} , cube \mathcal{C} , octahedron \mathcal{O} , dodecahedron \mathcal{D} and icosahedron \mathcal{I} are well-known [8,17,22], and are summarised in Table 2, where N_0, N_1 and N_2 denote

the numbers of vertices, edges and faces. A Schläfli symbol $\{m, n\}$ means that the faces are m -gons, n meeting at each vertex, so as a hypermap \mathcal{P} has type $(l_0, l_1, l_2) = (n, 2, m)$, since each edge meets two vertices and two faces.

\mathcal{P}	Schläfli	N_0	N_1	N_2	$\text{Aut } \mathcal{P}$	$\text{Aut}^+ \mathcal{P}$
\mathcal{T}	$\{3, 3\}$	4	6	4	S_4	A_4
\mathcal{O}	$\{3, 4\}$	6	12	8	$S_4 \times C_2$	S_4
\mathcal{C}	$\{4, 3\}$	8	12	6	$S_4 \times C_2$	S_4
\mathcal{I}	$\{3, 5\}$	12	30	20	$A_5 \times C_2$	A_5
\mathcal{D}	$\{5, 3\}$	20	30	12	$A_5 \times C_2$	A_5

Table 2. The five Platonic solids \mathcal{P} as hypermaps

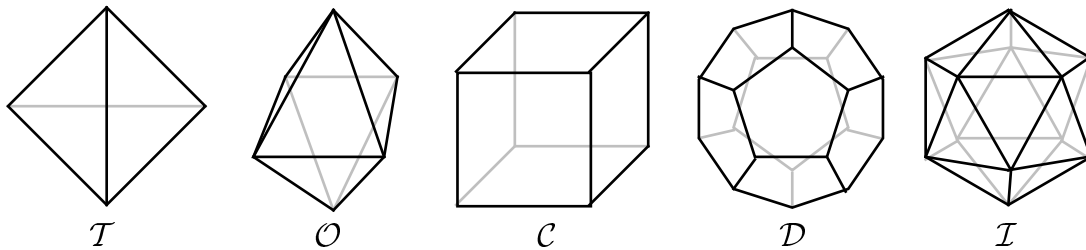


Figure 3.1. The five Platonic solids

The Platonic solids \mathcal{P} are illustrated (as convex polyhedra) in Figure 3.1. In each case we can regard \mathcal{P} as a spherical map, and we obtain a representation of \mathcal{P} as a (topological) hypermap by “thickening” the vertices and edges to give $2n$ - and 4 -sided regions on the sphere, representing the hypervertices and hyperedges; the complementary regions, which have $2m$ sides, are the hyperfaces. This is illustrated in Figure 3.2, where for convenience the sphere has been projected stereographically onto the plane \mathbf{R}^2 .

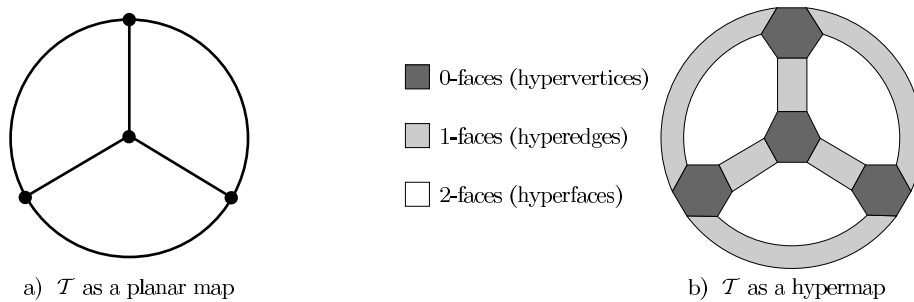
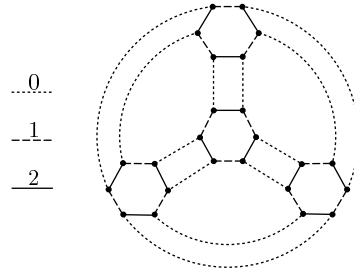


Figure 3.2. \mathcal{T} as a map and as a hypermap

In Figure 3.2(b) the black, grey and white regions are the i -faces of \mathcal{T} for $i = 0, 1$ and 2 , that is, the hypervertices, hyperedges and hyperfaces of \mathcal{T} , while the 24 vertices are the blades of \mathcal{T} . Figure 3.3 shows the underlying trivalent graph \mathcal{G} of \mathcal{T} , where each edge joining two i -faces is labelled i .

Figure 3.3. The underlying graph \mathcal{G} of \mathcal{T}

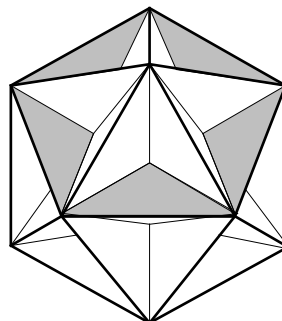
For each regular hypermap \mathcal{H} , the corresponding trivalent graph \mathcal{G} is the Cayley graph for $G = \text{Aut } \mathcal{H}$ with respect to a Δ -basis \mathbf{r} satisfying

$$r_i^2 = (r_1 r_2)^{l_0} = (r_2 r_0)^{l_1} = (r_0 r_1)^{l_2} = 1;$$

when \mathcal{H} is a Platonic solid \mathcal{P} these are defining relations for G , corresponding to the fact that \mathcal{P} is the universal map [10, Ch.8] or hypermap [7] of type (l_0, l_1, l_2) .

The automorphism group $\text{Aut } \mathcal{T}$ of \mathcal{T} (as a map, hypermap or convex polyhedron) is isomorphic to S_4 : the automorphisms induce all possible permutations of the four vertices, with the rotations inducing the even permutations, so $\text{Aut}^+ \mathcal{T} \cong A_4$. The dual pair \mathcal{C} and \mathcal{O} have automorphism groups $\text{Aut } \mathcal{C} \cong \text{Aut } \mathcal{O} \cong S_4 \times C_2$: the first factor is the rotation group, corresponding to the permutations of the four pairs of opposite vertices of \mathcal{C} (or faces of \mathcal{O}), and the second factor is generated by the antipodal symmetry. Similarly \mathcal{D} and its dual \mathcal{I} have automorphism group $A_5 \times C_2$: the 20 vertices of \mathcal{D} can be partitioned into five sets of four, each set the vertices of an inscribed tetrahedron, and the rotation group A_5 induces the even permutations of these tetrahedra; the antipodal symmetry generates the factor C_2 .

Another hypermap we shall need is the *great dodecahedron* \mathcal{GD} . This is Poincaré's star-polyhedron denoted by $\{5, \frac{5}{2}\}$ in [8, Ch.VI], which contains a detailed description of this and other star-polyhedra; \mathcal{GD} can be identified with the regular map $\{5, 5|3\}$ of type $\{5, 5\}$ and genus 4 in [10, §8.5] (see also [2, p.14; 26, pp. 19–22]). It has the 12 vertices and 30 edges of the icosahedron \mathcal{I} ; for each vertex v of \mathcal{I} the 5 neighbouring vertices lie on a circuit $(abcde)$ in \mathcal{I} , to which we attach a pentagonal face Φ_v of \mathcal{GD} . This is illustrated in Figure 3.4, where the visible part of one of the 12 faces of \mathcal{GD} is shaded; note that in this picture, faces intersect, so it does not represent an imbedding of \mathcal{GD} in \mathbf{R}^3 , though it does illustrate the fact that $\text{Aut } \mathcal{GD} \cong \text{Aut } \mathcal{I} \cong A_5 \times C_2$.

Figure 3.4. The great dodecahedron \mathcal{GD}

At v , 5 pentagons meet; a rotation on \mathcal{GD} once around v crosses edges in the cyclic order (va, vc, ve, vb, vd) , so it corresponds to a rotation twice around v on \mathcal{I} . (Thus \mathcal{GD} is the map $H_2(\mathcal{I})$ obtained by applying Wilson’s rotation-doubling operator H_2 to \mathcal{I} [30,20].) Using radial projection from the centre of \mathcal{I} , we see that \mathcal{GD} is a 3-sheeted covering of the sphere, with branch-points of order 1 at the 12 vertices v , where two sheets meet (the third sheet contains Φ_v). The vertex-figure at v is a pentagram $\{\frac{5}{2}\}$, which explains Coxeter’s symbol $\{5, \frac{5}{2}\}$ for \mathcal{GD} in [8]. Having 12 vertices, 30 edges and 12 faces, \mathcal{GD} has Euler characteristic $\chi = 12 - 30 + 12 = -6$; being a branched covering of the sphere \mathcal{GD} is orientable, so it has genus $g = 1 - \frac{1}{2}\chi = 4$. As a map, \mathcal{GD} is isomorphic to its dual, the small stellated dodecahedron $\{\frac{5}{2}, 5\}$ [8, Ch.6]. The two remaining Kepler-Poinsot star-polyhedra are the great stellated dodecahedron $\{\frac{5}{2}, 3\}$ and its reciprocal, the great icosahedron $\{3, \frac{5}{2}\}$; these are 7-sheeted coverings of the sphere, and as maps they are isomorphic to \mathcal{D} and \mathcal{I} respectively (see Figure 3.5, where a face is shaded in each case).

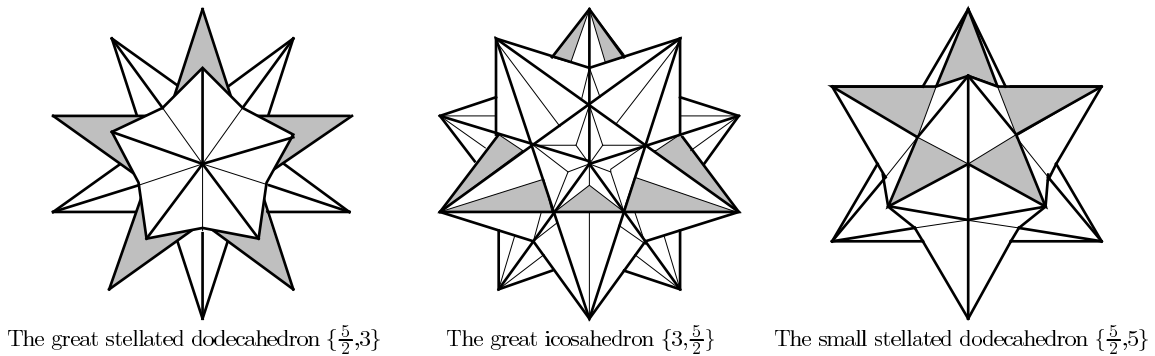


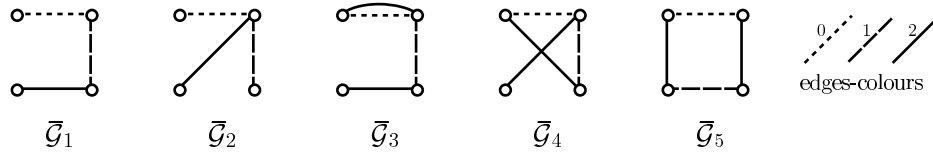
Figure 3.5. Star-polyhedra

4. Regular hypermaps with automorphism group S_4

4.1. Enumeration of the hypermaps

As explained at the end of §2, it will be convenient for us to use the natural representation of $G = S_4$ on $\{1, 2, 3, 4\}$, first determining the possible 4-vertex permutation graphs $\overline{\mathcal{G}}$ for G with respect to any Δ -basis $\mathbf{r} = (r_i)$ for G . Two Δ -bases \mathbf{r} and \mathbf{r}' give isomorphic hypermaps $\mathcal{H} \cong \mathcal{H}'$ if and only if they are equivalent under $\text{Aut } G$; since $\text{Aut } S_4 = \text{Inn } S_4 \cong S_4$ this is equivalent to the corresponding graphs $\overline{\mathcal{G}}$ and $\overline{\mathcal{G}'}$ differing only in their vertex-labels, so by omitting vertex-labels we obtain the isomorphism classes of regular S_4 -hypermaps. Similarly, by regarding the edges of $\overline{\mathcal{G}}$ as 3-coloured, with the colours to be replaced with the labels $i = 0, 1, 2$ in any of the $3!$ bijective ways, we obtain the orbits of S on these regular hypermaps.

There are two conjugacy classes of involutions in S_4 : the six transpositions, which are odd, are represented by single edges in $\overline{\mathcal{G}}$, while the three double-transpositions, which are even, are represented by disjoint pairs of edges. The double-transpositions lie in a Klein 4-group $V_4 \triangleleft S_4$, and since $|S_4 : V_4| > 2$ it follows that in order to generate S_4 at least two of the involutions r_i in \mathbf{r} must be transpositions. Since $\overline{\mathcal{G}}$ must be connected, it is easily seen that, up to graph-isomorphisms and permutations of edge-colours, the only possibilities for $\overline{\mathcal{G}}$ are among the graphs $\overline{\mathcal{G}}_1, \dots, \overline{\mathcal{G}}_5$ in Figure 4.1.

Figure 4.1. Possibilities for $\overline{\mathcal{G}}$ when $G \cong S_4$

In all five cases, the subgroup $\langle \mathbf{r} \rangle$ of S_4 generated by r_0, r_1 and r_2 is transitive and contains a transposition; in the cases $\overline{\mathcal{G}}_1, \dots, \overline{\mathcal{G}}_4$ it also contains a 3-cycle $(ab).(bc) = (acb)$, so it has order divisible by 4.3.2 and is therefore equal to S_4 . In the case of $\overline{\mathcal{G}}_5$, however, r_0, r_1 and r_2 visibly generate an imprimitive proper subgroup (D_4 , in fact). Thus there are four S -orbits on the regular S_4 -hypermaps, corresponding to $\overline{\mathcal{G}} = \overline{\mathcal{G}}_1, \dots, \overline{\mathcal{G}}_4$. In the case of $\overline{\mathcal{G}}_1$, this orbit has length $\sigma = 3$: by assigning a label $i = 0, 1$ or 2 to the right-hand edge we get three non-isomorphic hypermaps, since transposing the labels on the other two edges induces an isomorphism. Similarly $\overline{\mathcal{G}}_2, \overline{\mathcal{G}}_3$ and $\overline{\mathcal{G}}_4$ correspond to S -orbits of lengths $\sigma = 1, 6$ and 3 respectively. Thus there are, up to isomorphism, $3 + 1 + 6 + 3 = 13$ regular S_4 -hypermaps \mathcal{H} ; this agrees with P.Hall's result ([13], see also §8) that the number $d_\Delta(S_4)$ of normal subgroups $H \triangleleft \Delta$ with $\Delta/H \cong S_4$ is equal to 13.

4.2. Description of the hypermaps

By using Figure 4.1 to find the orders l_i of the permutations $r_j r_k$ ($\{i, j, k\} = \{0, 1, 2\}$), we see that, up to a reordering by S , \mathcal{H} has type $(l_0, l_1, l_2) = (3, 2, 3), (3, 3, 3), (4, 2, 3)$ and $(4, 4, 3)$ when $\overline{\mathcal{G}} = \overline{\mathcal{G}}_1, \dots, \overline{\mathcal{G}}_4$, and so \mathcal{H} has Euler characteristic $\chi = \frac{1}{2}|G|(\sum l_i^{-1} - 1) = 2, 0, -1, -2$ respectively.

The only subgroup of index 2 in S_4 is A_4 . In the cases $\overline{\mathcal{G}}_1$ and $\overline{\mathcal{G}}_2$ each r_i is odd, so \mathcal{H} is orientable, with rotation group $\text{Aut}^+ \mathcal{H} \cong A_4$, and \mathcal{H} has genus $g = 1 - \frac{1}{2}\chi = 0, 1$ respectively. When $\overline{\mathcal{G}} = \overline{\mathcal{G}}_3$ or $\overline{\mathcal{G}}_4$ some r_i is even, so \mathcal{H} is non-orientable of genus $g = 2 - \chi = 1$ or 4 .

This information is summarised in Table 3, where each row describes a representative S_4 -hypermap $\mathcal{H} = \mathcal{S}_r$ from the S -orbit corresponding to $\overline{\mathcal{G}} = \overline{\mathcal{G}}_r$ ($r = 1, \dots, 4$). The first column indicates the method of construction of \mathcal{S}_r , to be described in §4.3. The second column gives the size σ of the S -orbit containing \mathcal{S}_r , and the third gives its type (l_0, l_1, l_2) ; the types of the associates of \mathcal{S}_r are found by permuting the terms l_i . These associates all have the same Euler characteristic χ , orientability, and genus g , given in the last three columns (+ and - denoting orientable and non-orientable hypermaps, respectively).

\mathcal{H}	σ	N_0	N_1	N_2	χ	orient.	g
$\mathcal{S}_1 = \mathcal{T}$	3	3	2	3	2	+	0
$\mathcal{S}_2 = W^{-1}(\mathcal{T}^{\hat{0}})$	1	3	3	3	0	+	1
$\mathcal{S}_3 = \mathcal{PO}$	6	4	2	3	1	-	1
$\mathcal{S}_4 = W^{-1}(\mathcal{PO}^{\hat{0}})$	3	4	4	3	-2	-	4

Table 3. The 13 regular hypermaps \mathcal{H} with $\text{Aut } \mathcal{H} \cong S_4$

4.3. Construction of the hypermaps

The first row in Table 3, corresponding to $\overline{\mathcal{G}}_1$, gives an S -orbit of three orientable hypermaps \mathcal{H} of genus 0. The chosen representative \mathcal{S}_1 is the tetrahedron \mathcal{T} , which is a map of type $\{3, 3\}$ and thus a hypermap of type $(3, 2, 3)$; Figure 3.2 shows \mathcal{T} drawn as a map and as a hypermap. Now \mathcal{T} is self-dual (that is, $\mathcal{T} \cong \mathcal{T}^{(02)}$), so this orbit of S has length $\sigma = 3$ rather than 6; the other two associates of \mathcal{T} are $\mathcal{T}^{(01)}$ and $\mathcal{T}^{(12)}$, spherical hypermaps of types $(2, 3, 3)$ and $(3, 3, 2)$ obtained from \mathcal{T} by transposing hyperedges with hypervertices and hyperfaces respectively. For example, Figure 4.2 shows two drawings of $\mathcal{T}^{(12)}$, with hypervertices, hyperedges and hyperfaces black, grey and white; it also shows the Walsh map $W(\mathcal{T}^{(12)})$, with black and white vertices corresponding to the hypervertices and hyperedges of $\mathcal{T}^{(12)}$.

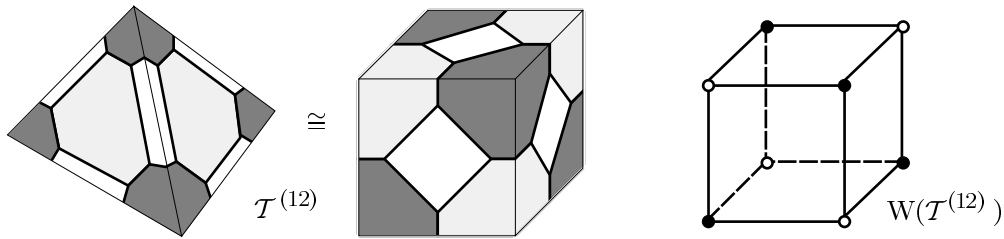


Figure 4.2. The hypermap $\mathcal{T}^{(12)}$ and its Walsh map

The second S -orbit, corresponding to $\overline{\mathcal{G}}_2$, consists of a single S -invariant orientable hypermap $\mathcal{H} = \mathcal{S}_2$ of type $(3, 3, 3)$ and genus 1; it has four hypervertices, four hyperedges and four hyperfaces. We can construct \mathcal{S}_2 from \mathcal{T} using the method outlined in §2 (see also [4]). Being a non-bipartite regular map of type $\{3, 3\}$, \mathcal{T} has a bipartite double cover $\mathcal{T}^{\hat{0}} = \mathcal{T} \times \mathcal{B}^{\hat{0}}$ which is the Walsh map $W(\mathcal{S}_2)$ of some regular hypermap $\mathcal{S}_2 = W^{-1}(\mathcal{T}^{\hat{0}})$ of type $(3, 3, 3)$, with $\text{Aut } \mathcal{S}_2 \cong \text{Aut } \mathcal{T} \cong S_4$. The underlying surface of \mathcal{S}_2 is a torus (Figure 4.3); as a double covering of the sphere, it is branched at the four face-centres of \mathcal{T} . The construction of \mathcal{S}_2 is described in detail in [4, §1], where it is denoted by \mathcal{T}' ; one can also obtain \mathcal{S}_2 by putting $b = 2, c = 0$ in Theorem 12 of [7].

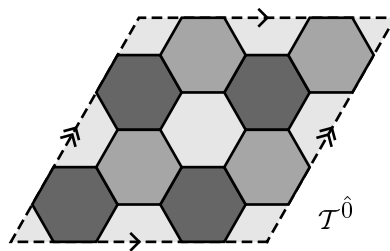


Figure 4.3. The hypermap \mathcal{S}_2 on a torus

The third S -orbit, corresponding to $\overline{\mathcal{G}}_3$, consists of six non-orientable hypermaps, including the *projective octahedron* $\mathcal{S}_3 = P\mathcal{O}$, which we will now construct. The octahedron \mathcal{O} is a regular spherical hypermap of type $(4, 2, 3)$ with $\text{Aut } \mathcal{O} \cong S_4 \times C_2$; these two factors represent the rotation group and the subgroup generated by the antipodal automorphism. By identifying antipodal points of \mathcal{O} one obtains a regular hypermap $P\mathcal{O} = \mathcal{O}/C_2$ of type

$(4, 2, 3)$ on the projective plane, with $\text{Aut } P\mathcal{O} \cong S_4$; this is the map $\{3, 4\}/2 = \{3, 4\}_3$ of [10, §8.6], shown in Figure 4.4 where opposite boundary points are identified.

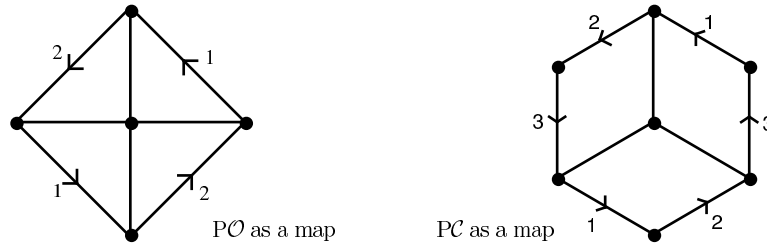


Figure 4.4. The hypermaps $P\mathcal{O}$ and $P\mathcal{C}$

There are three hypervertices, six hyperedges, and four hyperfaces. Among the associates of $P\mathcal{O}$ is its dual $(P\mathcal{O})^{(02)} = P(\mathcal{O}^{(02)}) = P\mathcal{C}$, the *projective cube*, also shown in Figure 4.4. This is the regular map $\{4, 3\}/2 = \{4, 3\}_3$ of [10, §8.6], sometimes called the Purse of Fortunatus [9]; it is an interesting experiment to take three square handkerchiefs and try sewing them together to form $P\mathcal{C}$!

The last S -orbit, corresponding to $\overline{\mathcal{G}}_4$, contains three non-orientable hypermaps of characteristic -2 ; the chosen representative $\mathcal{S}_4 = W^{-1}(P\mathcal{O}^{\hat{0}})$, of type $(4, 4, 3)$, is formed from $\mathcal{S}_3 = P\mathcal{O}$ in the same way as $\mathcal{S}_2 = W^{-1}(\mathcal{T}^{\hat{0}})$ is formed from $\mathcal{S}_1 = \mathcal{T}$: it is the hypermap whose Walsh map $W(\mathcal{S}_4)$ is the bipartite double covering $P\mathcal{O}^{\hat{0}}$ of the non-bipartite map $P\mathcal{O}$ (see Figure 4.5).

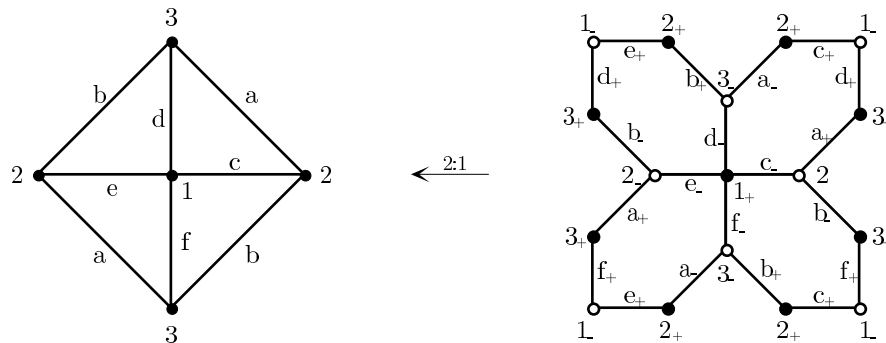


Figure 4.5. $P\mathcal{O}$ covered by $P\mathcal{O}^{\hat{0}} = W(\mathcal{S}_4)$

This is a double covering of the projective plane, branched at the four face-centres of $P\mathcal{O}$. Thus each of the four triangular faces of $P\mathcal{O}$ lifts to a hexagonal face of $P\mathcal{O}^{\hat{0}}$, representing a hyperface of \mathcal{S}_4 ; each of the three vertices $1, 2, 3$ of $P\mathcal{O}$ lifts to a pair $1_+, 1_-$ etc. of vertices of $P\mathcal{O}^{\hat{0}}$, coloured black and white and representing a hypervertex and a hyperedge of \mathcal{S}_4 respectively. Each edge a, \dots, f of $P\mathcal{O}$ lifts to a pair a_+, a_- etc. of edges of $P\mathcal{O}^{\hat{0}}$. The covering $P\mathcal{O}^{\hat{0}} \rightarrow P\mathcal{O}$ is shown in Figure 4.5, where pairs of boundary edges with the same label are identified, as indicated by their incident vertices; thus horizontal and vertical boundary edges of $P\mathcal{O}^{\hat{0}}$ (labelled c_+, d_+, e_+, f_+) are identified orientably, as in the construction of a torus from a square, while diagonal boundary edges (labelled a_+, a_-, b_+, b_-) are identified non-orientably, so the underlying surface is a torus with two cross-caps. The resulting hypermap \mathcal{S}_4 is shown in Figure 4.6, where the identification of sides of the 12-gon is indicated by the surface-symbol

$(abcdeb^{-1}afe^{-1}dc^{-1}f^{-1})$: thus the pair of sides labelled a, a are joined non-orientably, while b, b^{-1} indicates an orientable join, etc.

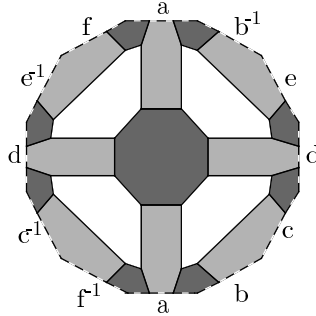


Figure 4.6. The hypermap \mathcal{S}_4

This completes the construction of the 13 regular S_4 -hypermaps; note that four of them are orientable, and three are maps (namely $\mathcal{T}, P\mathcal{O}$ and PC).

5. Regular hypermaps with automorphism group A_5

5.1. Enumeration of the hypermaps

We will represent elements of $G = A_5$ as even permutations of $\{1, \dots, 5\}$, so $\bar{\mathcal{G}}$ is now a 5-vertex graph. Since $\text{Aut } A_5 \cong S_5$, isomorphism classes of regular A_5 -hypermaps \mathcal{H} correspond to unlabelled permutation graphs $\bar{\mathcal{G}}$, as in §4 for S_4 .

The 15 involutions in A_5 are all conjugate; being double-transpositions, they are represented as disjoint pairs of edges in $\bar{\mathcal{G}}$. It is not hard to see that (up to graph-isomorphisms and permutations of the edge-colours) the only connected permutation graphs $\bar{\mathcal{G}}$ for three double-transpositions $r_i \in A_5$ are those shown in Figure 5.1.

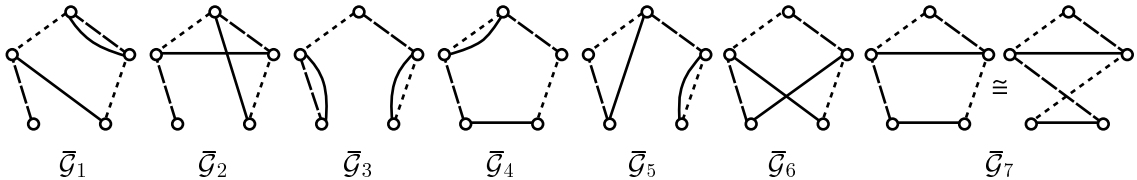


Figure 5.1. Possibilities for $\bar{\mathcal{G}}$ when $G \cong A_5$

Being transitive, the subgroup $\langle \mathbf{r} \rangle$ of A_5 generated by r_0, r_1 and r_2 has order divisible by 5. In the cases $\bar{\mathcal{G}}_1, \dots, \bar{\mathcal{G}}_5$ one can inspect $\bar{\mathcal{G}}$ to find an element of order 3 in $\langle \mathbf{r} \rangle$, so $\langle \mathbf{r} \rangle$ has order divisible by 15 and must therefore be A_5 . In the final case, however, the second drawing of $\bar{\mathcal{G}}_7$ shows that there is a cyclic ordering of the vertices inverted by each r_i , so $\langle \mathbf{r} \rangle \cong D_5$. Thus there are six S -orbits of regular A_5 -hypermaps \mathcal{H} , corresponding to $\bar{\mathcal{G}} = \bar{\mathcal{G}}_1, \dots, \bar{\mathcal{G}}_6$. By considering which permutations of edge-labels induce graph-isomorphisms, we see that these S -orbits have lengths 6, 3, 3, 3, 3 and 1 respectively, so there are, up to isomorphism, 19 regular A_5 -hypermaps \mathcal{H} (in accordance with P.Hall’s result [13] that $d_\Delta(A_5) = 19$, see §8).

5.2. Description of the hypermaps

Since A_5 has no subgroup of index 2, all 19 hypermaps \mathcal{H} are non-orientable. By inspecting each $\overline{\mathcal{G}} = \overline{\mathcal{G}}_1, \dots, \overline{\mathcal{G}}_6$ one can compute the type and hence the Euler characteristic χ and genus g of each \mathcal{H} , as in §4.2. This information is given in Table 4, where, as in Table 3 for $G = S_4$, each row describes a representative $\mathcal{H} = \mathcal{A}_r$ chosen from the S -orbit of length σ corresponding to $\overline{\mathcal{G}}_r$ ($r = 1, \dots, 6$). Notice that $\overline{\mathcal{G}}_4$ and $\overline{\mathcal{G}}_5$ both yield hypermaps of type $(5, 5, 3)$; they are not isomorphic since $r_0 r_1 r_0 r_2$ has order 2 and 3 respectively (alternatively, the elements $r_1 r_2$ and $r_2 r_0$ of order 5 are conjugate and not conjugate respectively).

\mathcal{H}	σ	N_0	N_1	N_2	χ	orient.	g
$A_1 = PD$	6	3	2	5	1	–	1
$A_2 = PGD$	3	5	2	5	–3	–	5
$A_3 = W^{-1}(PD^{\hat{0}})$	3	3	3	5	–4	–	6
$A_4 = W^{-1}(PI^{\hat{0}})$	3	5	5	3	–8	–	10
$A_5 = PA_5^{\dagger}$	3	5	5	3	–8	–	10
$A_6 = W^{-1}(PGD^{\hat{0}})$	1	5	5	5	–12	–	14

Table 4. The 19 regular hypermaps \mathcal{H} with $\text{Aut } \mathcal{H} \cong A_5$

5.3. Construction of the hypermaps

The first S -orbit, corresponding to $\overline{\mathcal{G}}_1$, is represented by the *projective dodecahedron* $\mathcal{A}_1 = PD = \mathcal{D}/C_2$; this is the regular map $\{5, 3\}/2$ on the projective plane formed by identifying antipodal points of the dodecahedron \mathcal{D} , and is also the map $\{5, 3\}_5$ of [10, §8.6]. This S -orbit also contains its dual, the *projective icosahedron* $\mathcal{A}_1^{(02)} = PI = \mathcal{I}/C_2 = \{3, 5\}_5$. Both maps are shown in Figure 5.2, where opposite boundary points are identified to form the projective plane.

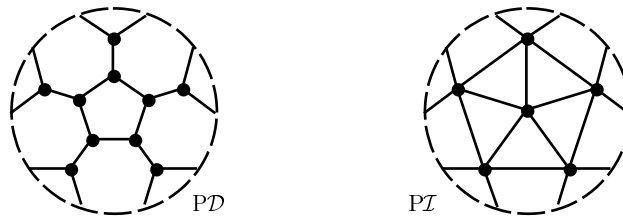


Figure 5.2. The hypermaps PD and PI

Similarly, the great dodecahedron \mathcal{GD} , an orientable regular map of type $\{5, 5\}$ and genus 4 shown in Figure 3.4, yields a non-orientable regular map \mathcal{A}_2 of type $\{5, 5\}$ and genus 5; this is the *projective great dodecahedron* $PGD = \mathcal{GD}/C_2$, isomorphic to $\{5, 5\}_3$ in [10, §8.6], lying in the S -orbit of length $\sigma = 3$ corresponding to $\overline{\mathcal{G}}_2$. This map is shown in Figure 5.3, where boundary edges are identified in pairs as indicated by the labelling of the vertices. Just as PD and PI are related by duality, PGD and PI are related by Wilson’s Petrie operation [29; 10, §8.6; 20], which transposes faces and Petrie polygons of maps while preserving the 1-skeleton.

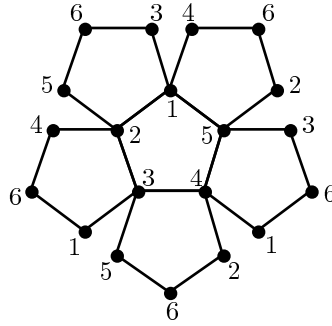


Figure 5.3. The hypermap $\mathcal{A}_2 = PG\mathcal{D}$

The projective dodecahedron PD is a non-bipartite map of type $\{5, 3\}$, so its bipartite double cover $PD^{\hat{0}} = PD \times \mathcal{B}^{\hat{0}}$ is the Walsh map of a hypermap $\mathcal{A}_3 = W^{-1}(PD^{\hat{0}})$ of type $(3, 3, 5)$; like PD , \mathcal{A}_3 is regular, with $\text{Aut } \mathcal{A}_3 \cong \text{Aut } PD \cong A_5$. Its underlying surface is a non-orientable double covering of the projective plane, branched at the six face-centres of PD , so it has characteristic $2 \cdot 1 - 6 = -4$ and genus 6. The Walsh map $W(\mathcal{A}_3) = PD^{\hat{0}}$ is shown in Figure 5.4, with black and white vertices representing the hypervertices and hyperedges of \mathcal{A}_3 ; part of the surface symbol $(ab \dots cb \dots cd \dots ad \dots)$ is shown, indicating the identifications needed to form the shaded face; rotation about the centre gives four more faces, similarly formed, and the central face completes the six faces of $PD^{\hat{0}}$, corresponding to the six hyperfaces of \mathcal{A}_3 .

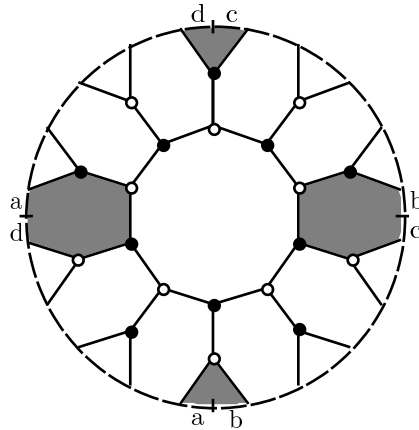


Figure 5.4. The map $W(\mathcal{A}_3) = PD^{\hat{0}}$

Rotation of Figure 5.4 through π about its centre induces an automorphism of order 2 of $PD^{\hat{0}}$, interchanging the sets of black and white vertices; this shows that $\mathcal{A}_3 \cong \mathcal{A}_3^{(01)}$, so the S -orbit containing \mathcal{A}_3 has length $\sigma = 3$. The quotient of $PD^{\hat{0}}$ by this automorphism is the map PD shown in Figure 5.2.

Similarly, the non-bipartite maps PI and $PG\mathcal{D}$ of types $\{3, 5\}$ and $\{5, 5\}$ give rise to non-orientable regular A_5 hypermaps $\mathcal{A}_4 = W^{-1}(PI^{\hat{0}})$ and $\mathcal{A}_6 = W^{-1}(PG\mathcal{D}^{\hat{0}})$ of types $(5, 5, 3)$ and $(5, 5, 5)$, corresponding to $\overline{\mathcal{G}}_4$ and $\overline{\mathcal{G}}_6$. The underlying surface of \mathcal{A}_4 is a double covering of the projective plane, branched at the 10 face-centres of PI , so it has characteristic $2 \cdot 1 - 10 = -8$ and genus 10. Figure 5.5 shows $W(\mathcal{A}_4) = PI^{\hat{0}}$ as a bipartite double covering of PI : the vertex-labelling and colouring indicate the identifications of boundary edges. Since

$\mathcal{A}_4 \cong \mathcal{A}_4^{(01)}$ we have $\sigma = 3$ for this S -orbit.

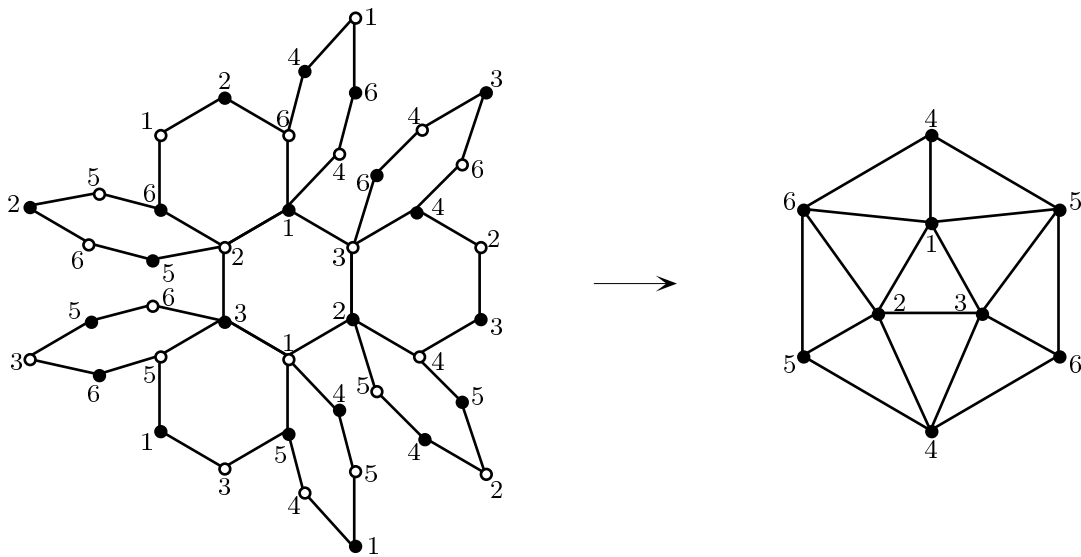


Figure 5.5. The double covering $W(\mathcal{A}_4) = PT^{\hat{0}} \rightarrow PI$

In the case of \mathcal{A}_6 , the surface is a double covering of $P\mathcal{G}\mathcal{D}$ (which has characteristic -3), branched at the 6 face-centres, so it has characteristic $2 \cdot (-3) - 6 = -12$ and genus 14. Figure 5.6 shows $W(\mathcal{A}_6) = P\mathcal{G}\mathcal{D}^{\hat{0}}$ as a branched double covering of the map $P\mathcal{G}\mathcal{D}$ in Figure 5.3. Being the unique regular A_5 -hypermap of type $(5, 5, 5)$, \mathcal{A}_6 is S -invariant, that is, its S -orbit has length $\sigma = 1$.

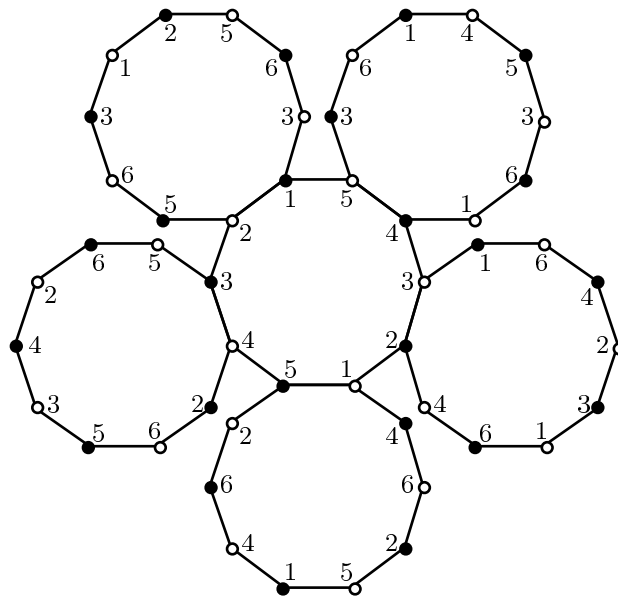


Figure 5.6. The map $W(\mathcal{A}_6) = P\mathcal{G}\mathcal{D}^{\hat{0}}$

Like $\overline{\mathcal{G}}_4$, $\overline{\mathcal{G}}_5$ corresponds to an S -orbit of length 3 containing a non-orientable hypermap of type $(5, 5, 3)$ and genus 10, namely \mathcal{A}_5 . However, $\mathcal{A}_5 \not\cong \mathcal{A}_4$: when $\overline{\mathcal{G}} = \overline{\mathcal{G}}_4$ the elements $r_1 r_2$ and $r_2 r_0$ (which rotate all blades around hypervertices and hyperedges) are conjugate in A_5 ,

since by inspection $r_2r_0 = (r_1r_2)^{r_0r_1}$; when $\bar{\mathcal{G}} = \bar{\mathcal{G}}_5$, on the other hand, each of r_1r_2 and r_2r_0 is conjugate in A_5 to the square of the other, so they are conjugate in S_5 but not in A_5 . To see that $W^{-1}(P\mathcal{I}^{\hat{0}})$ is isomorphic to \mathcal{A}_4 and not \mathcal{A}_5 , note that in Figure 5.5 the rotations around the black and white vertices of $P\mathcal{I}^{\hat{0}}$ are both lifted from the same rotations around the vertices of $P\mathcal{I}$, so r_1r_2 and r_2r_0 are conjugate. An alternative way of distinguishing \mathcal{A}_4 from \mathcal{A}_5 (and of showing that $W^{-1}(P\mathcal{I}^{\hat{0}}) \cong \mathcal{A}_4$) is to note that $r_0r_1r_0r_2$ has order 2 and 3 respectively in these two maps.

We will construct \mathcal{A}_5 from the Walsh map of its orientable double cover \mathcal{A}_5^+ . First we construct a bipartite orientable map \mathcal{M}_5 , then we take \mathcal{A}_5^+ to be the corresponding hypermap $W^{-1}(\mathcal{M}_5)$, a regular orientable hypermap with $\text{Aut } \mathcal{A}_5^+ \cong A_5 \times C_2$, and finally we take \mathcal{A}_5 to be the antipodal quotient $P\mathcal{A}_5^+ = \mathcal{A}_5^+/C_2$, a non-orientable regular A_5 -hypermap. (It is straightforward to check that $W^{-1}(\mathcal{M}_5)$ is the orientable double cover of \mathcal{A}_5 , so the notation \mathcal{A}_5^+ is justified.) We take the 1-skeleton of \mathcal{M}_5 to be that of $\mathcal{I}^{\hat{0}}$, or equivalently of the small stellated triacontahedron shown in Figure 6.3: each vertex v of \mathcal{I} corresponds to a pair v_+ and v_- of black and white vertices of \mathcal{M}_5 , and each edge vw of \mathcal{I} corresponds to two edges v_+w_- and v_-w_+ of \mathcal{M}_5 . This gives us a connected bipartite 5-valent graph with 24 vertices and 60 edges. For each face (uvw) of \mathcal{I} we take a six-sided face $(u_-z_+v_-x_+w_-y_+)$, as shown in Figure 5.7, where x, y and z are the other vertices of \mathcal{I} adjacent to v and w , to w and u , and to u and v respectively.

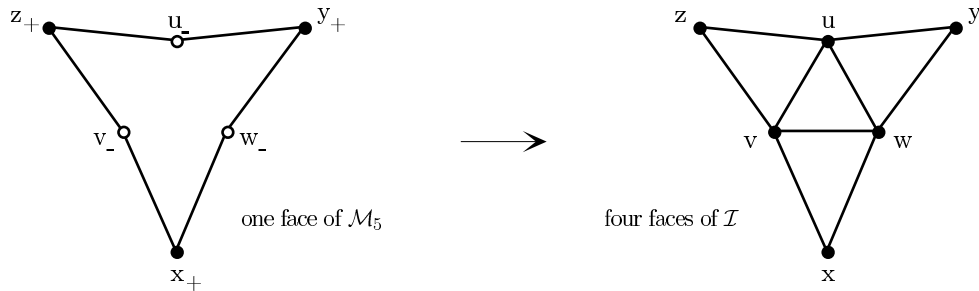


Figure 5.7. A face of \mathcal{M}_5

We now have an orientable bipartite map \mathcal{M}_5 with 20 hexagonal faces. Figure 5.7 shows that each face of \mathcal{I} is covered by four faces of \mathcal{M}_5 , so the surface of \mathcal{M}_5 is a 4-sheeted covering of the sphere, with branch-points of order 2 at the 12 white vertices v_- : Figure 5.8 shows that if an orientation of \mathcal{I} induces the cyclic order $\rho = (abcde)$ of neighbouring vertices of v in \mathcal{I} , then around v_+ the order is $(a_-b_-c_-d_-e_-)$, giving a single unbranched sheet, whereas around v_- the order is $(a_+d_+b_+e_+c_+)$, so three sheets are joined to give a branch-point of order 2, as in Figure 5.9.

Being bipartite, \mathcal{M}_5 is the Walsh map of an orientable hypermap $\mathcal{A}_5^+ = W^{-1}(\mathcal{M}_5)$ of type $(5, 5, 3)$ and characteristic -16 : the 12 hypervertices, 12 hyperedges and 20 hyperfaces of \mathcal{A}_5^+ correspond to the black vertices, white vertices and faces of \mathcal{M}_5 . By the symmetry of the method of construction, $\text{Aut } \mathcal{A}_5^+$ contains $\text{Aut } \mathcal{I} \cong A_5 \times C_2$, of order 120; since \mathcal{A}_5^+ has 120 blades (two for each edge of \mathcal{M}_5), \mathcal{A}_5^+ must be regular, with $\text{Aut } \mathcal{A}_5^+ \cong A_5 \times C_2$. The antipodal factor C_2 induces an orientation-reversing fixed-point-free automorphism of \mathcal{A}_5^+ , and the

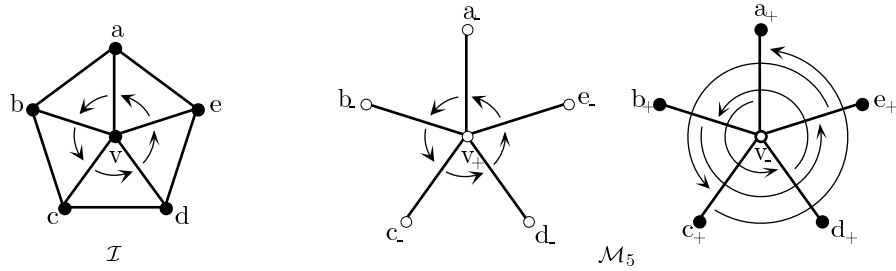


Figure 5.8. Rotations around vertices of \mathcal{I} and \mathcal{M}_5

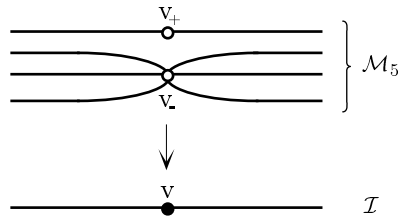


Figure 5.9. Branching of \mathcal{M}_5 over \mathcal{I}

quotient is a non-orientable regular A_5 -hypermap $\mathcal{A}_5 = \mathcal{A}_5^+/C_2 = W^{-1}(\mathcal{M}_5/C_2)$ of type $(5, 5, 3)$ and characteristic -8 . Equivalently, one can construct \mathcal{M}_5/C_2 directly from the 1-skeleton of $PI^{\hat{0}}$ by adding 6-sided faces as in Figure 5.7, and then define $\mathcal{A}_5 = W^{-1}(\mathcal{M}_5/C_2)$, as shown in Figure 5.10. (An alternative construction for \mathcal{A}_5^+ – and hence for \mathcal{A}_5 – is to take

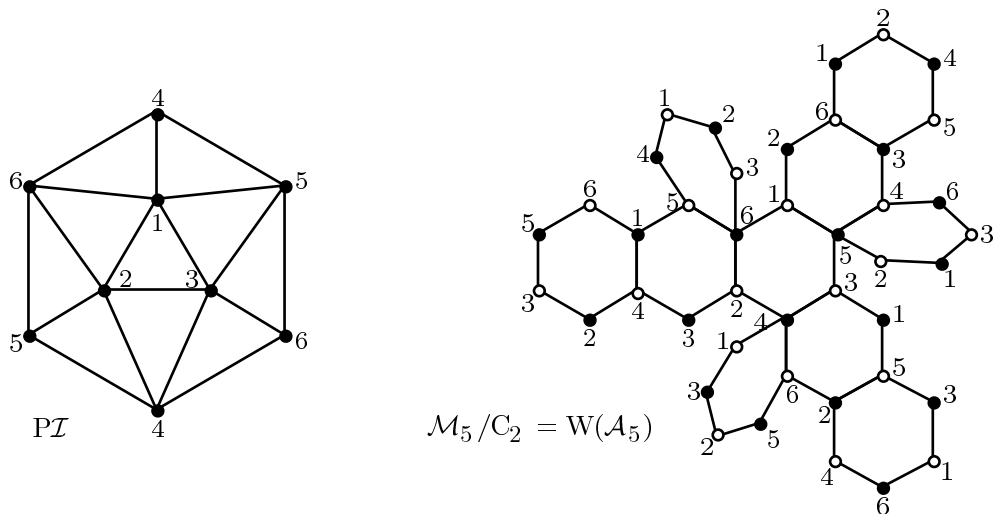


Figure 5.10. The construction of $W(\mathcal{A}_5)$ from PI

the graph Γ consisting of the 20 vertices and 60 face-diagonals of the dodecahedron \mathcal{D} ; each of the 12 faces Φ of \mathcal{D} carries a pentagram in Γ , to which we attach a disc representing a hyperedge Φ_- of \mathcal{A}_5^+ (see Figure 5.11(a)); the vertices of \mathcal{D} adjacent in \mathcal{D} to those in Φ form a pentagon in Γ , to which we attach a disc representing a hypervertex Φ_+ of \mathcal{A}_5^+ (see Figure 5.11(b)). This gives us a 2-face-coloured map – the dual of \mathcal{M}_5 – from which we obtain \mathcal{A}_5^+

by expanding each of the 20 vertices to a small disc representing a hyperface, incident with three hypervertices and three hyperedges.)

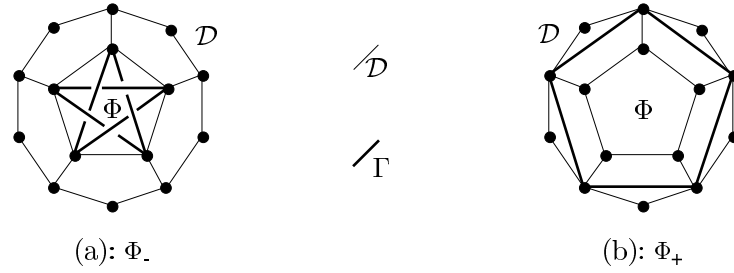


Figure 5.11. Φ_- and Φ_+

Using either of these two models, it is now easily seen that \mathcal{A}_5 corresponds to $\overline{\mathcal{G}}_5$ rather than $\overline{\mathcal{G}}_4$. For example, in \mathcal{A}_5^\pm the permutations $r_1 r_2$ and $r_2 r_0$ of order 5 around hypervertices and hyperedges correspond to rotations ρ and ρ^2 by angles $2\pi/5$ and $4\pi/5$ about vertices of \mathcal{I} (see Figures 5.8 and 5.11), so they are not conjugate in $A_5 \times C_2$; when we factor out C_2 , \mathcal{A}_5 also has this property. Alternatively, one can consider the action on the blades of the element $g = r_0 r_1 r_0 r_2$, shown in Figure 5.12, where we regard a blade as an incident edge-face pair in the Walsh map.

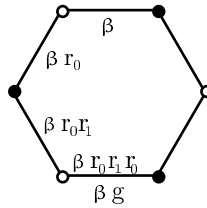


Figure 5.12. The action of $g = r_0 r_1 r_0 r_2$ on a blade β

We see from Figure 5.5 that g has order 2 on \mathcal{A}_4 , whereas Figure 5.10 shows that g has order 3 on \mathcal{A}_5 , confirming that \mathcal{A}_5 corresponds to $\overline{\mathcal{G}}_5$.

Having constructed $\mathcal{A}_1, \dots, \mathcal{A}_6$, we have now accounted for all 19 regular A_5 -hypermaps in Table 4. Among these, there are three maps: the projective dodecahedron $PD = \mathcal{A}_1$, the projective icosahedron $PI = \mathcal{A}_1^{(02)}$, and the projective great dodecahedron $PGD = \mathcal{A}_2$.

6. Regular hypermaps with automorphism group $A_5 \times C_2$

6.1. Enumeration of the hypermaps

In this case the hypermap subgroups are the normal subgroups $H \leq \Delta$ with $\Delta/H \cong G = A_5 \times C_2$; these are the intersections $H = A \cap B$ of normal subgroups A, B of Δ with $\Delta/A \cong A_5$ and $\Delta/B \cong C_2$, so the hypermaps \mathcal{H} we require are the disjoint products $\mathcal{H} = \mathcal{A} \times \mathcal{B}$ of regular hypermaps \mathcal{A} and \mathcal{B} with automorphism groups A_5 and C_2 . Since G decomposes as $A_5 \times C_2$ in a unique way, each H determines A and B uniquely, so each \mathcal{H} corresponds to a unique pair \mathcal{A}, \mathcal{B} . By §5 there are 19 possible hypermaps \mathcal{A} , and by §4 of [4] there are 7 possibilities for \mathcal{B} , so we obtain $19 \cdot 7 = 133$ hypermaps \mathcal{H} .

6.2. Description of the hypermaps

The 2-blade hypermaps \mathcal{B} are (where $\{i, j, k\} = \{0, 1, 2\}$):

- \mathcal{B}^+ , in which R_i, R_j and R_k transpose the two blades;
- \mathcal{B}^i , in which R_i fixes the two blades while R_j, R_k transpose them;
- $\mathcal{B}^{\hat{i}}$, in which R_i transposes the two blades while R_j, R_k fix them.

The 19 regular A_5 -hypermaps \mathcal{A} in §5 are all non-orientable and without boundary, so it follows from [4, §5] that their double coverings $\mathcal{H} = \mathcal{A} \times \mathcal{B}$ are without boundary, and that of these $\mathcal{A}^+ = \mathcal{A} \times \mathcal{B}^+$ is orientable, with rotation group $\text{Aut}^+ \mathcal{A}^+ \cong A_5$, while $\mathcal{A}^i = \mathcal{A} \times \mathcal{B}^i$ and $\mathcal{A}^{\hat{i}} = \mathcal{A} \times \mathcal{B}^{\hat{i}}$ are non-orientable. This gives us 19 orientable hypermaps $\mathcal{H} = \mathcal{A}^+$, and 114 non-orientable hypermaps $\mathcal{H} = \mathcal{A}^i$ and $\mathcal{A}^{\hat{i}}$ ($i = 0, 1, 2$).

If \mathcal{A} has type (l, m, n) then so has \mathcal{A}^+ : it is, in fact, the orientable double cover of \mathcal{A} , so that \mathcal{A} is the antipodal quotient $P\mathcal{A}^+ = \mathcal{A}^+/C_2$. Since \mathcal{B}^0 and $\mathcal{B}^{\hat{0}}$ have type $(1, 2, 2)$, \mathcal{A}^0 and $\mathcal{A}^{\hat{0}}$ have type $(l, m'n')$, where $m' = \text{lcm}(m, 2)$ and $n' = \text{lcm}(n, 2)$; similarly, \mathcal{A}^1 and $\mathcal{A}^{\hat{1}}$ have type (l', m', n') , while \mathcal{A}^2 and $\mathcal{A}^{\hat{2}}$ have type (l', m', n) .

Being an unbranched double covering of \mathcal{A} , \mathcal{A}^+ has characteristic $2\chi(\mathcal{A})$ and hence has genus $1 - \chi(\mathcal{A})$. The coverings $\mathcal{H} = \mathcal{A}^0$ and $\mathcal{A}^{\hat{0}}$ have branch-points of order 1 on the $30/m$ hyperedges of \mathcal{A} if m is odd, and on the $30/n$ hyperfaces if n is odd, with similar conditions on l and n for \mathcal{A}^1 and $\mathcal{A}^{\hat{1}}$, and on l and m for \mathcal{A}^2 and $\mathcal{A}^{\hat{2}}$. In each of these six cases we can therefore compute $\chi(\mathcal{H}) = 2\chi(\mathcal{A}) - \beta$ where β is the total order of branching; being non-orientable, \mathcal{H} has genus $2 - \chi(\mathcal{H})$.

	\mathcal{A}_r^+						$\mathcal{A}_r^0, \mathcal{A}_r^{\hat{0}}$						$\mathcal{A}_r^1, \mathcal{A}_r^{\hat{1}}$						$\mathcal{A}_r^2, \mathcal{A}_r^{\hat{2}}$					
	σ	N_0	N_1	N_2	+/-	g	σ	N_0	N_1	N_2	+/-	g	σ	N_0	N_1	N_2	+/-	g	σ	N_0	N_1	N_2	+/-	g
A_1	6	3	2	5	+	0	6	3	2	10	-	6	6	6	2	10	-	16	6	6	2	5	-	10
A_2	3	5	2	5	+	4	6	5	2	10	-	14	3	10	2	10	-	20	6	10	2	5	-	14
A_3	3	3	3	5	+	5	6	3	6	10	-	26	6	6	3	10	-	26	3	6	6	5	-	30
A_4	3	5	5	3	+	9	6	5	10	6	-	34	6	10	5	6	-	34	3	10	10	3	-	30
A_5	3	5	5	3	+	9	6	5	10	6	-	34	6	10	5	6	-	34	3	10	10	3	-	30
A_6	1	5	5	5	+	13	3	5	10	10	-	38	3	10	5	10	-	38	3	10	10	5	-	38

Table 5. The 133 regular hypermaps \mathcal{H} with $\text{Aut } \mathcal{H} \cong A_5 \times C_2$

This information is summarised in Table 5, where the six rows correspond to the six S -orbits (of length σ) on the regular A_5 -hypermaps \mathcal{A} , each orbit being represented by \mathcal{A}_r as in §5, while the columns correspond to the 2-blade hypermaps \mathcal{B}^+ , \mathcal{B}^0 and $\mathcal{B}^{\hat{0}}$, \mathcal{B}^1 and $\mathcal{B}^{\hat{1}}$, and \mathcal{B}^2 and $\mathcal{B}^{\hat{2}}$. Thus each entry in the column headed \mathcal{A}_r^+ corresponds to a single S -orbit, while the entries in the remaining three columns correspond to pairs of S -orbits.

6.3. Construction of the hypermaps

Row 1. The first row of Table 5 gives the 42 double coverings of $\mathcal{A}_1 = PD$ and their associates. The first entry represents the orientable double cover $(PD)^+ = \mathcal{D}$ of type $(3, 2, 5)$, together with its five associates, including the icosahedron $\mathcal{I} = \mathcal{D}^{(02)}$ of type $(5, 2, 3)$.

The second entry represents a pair of hypermaps PD^0 and $PD^{\hat{0}}$, both non-orientable, of type $(3, 2, 10)$ and characteristic -4 , together with their 10 associates. Both PD^0 and $PD^{\hat{0}}$ arise as double coverings of PD with branch-points at the six face-centres, but they are not isomorphic since they have different patterns of cuts between these branch-points. For example the map $PD^{\hat{0}}$, projecting onto $\mathcal{B}^{\hat{0}}$, is bipartite, whereas PD^0 is not. Alternatively, the permutation $g = r_0 r_1 r_2$, having orders 5, 1 and 2 in PD, \mathcal{B}^0 and $\mathcal{B}^{\hat{0}}$, has orders 5 and 10 in PD^0 and $PD^{\hat{0}}$ respectively, so $PD^0 \not\cong PD^{\hat{0}}$. In fact, this shows that the Petrie polygons of the maps PD^0 and $PD^{\hat{0}}$ have lengths 5 and 10, since g is the basic “zig” (or “zag”) from which such paths are formed; see Figure 6.1 for a typical Petrie polygon in PD .

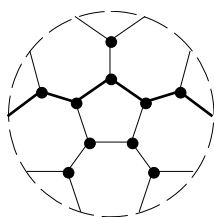


Figure 6.1. A Petrie polygon in PD

(This also shows that PD^0 can be formed by applying Wilson’s Petrie operation [29] to \mathcal{D} , transposing faces and Petrie polygons while retaining the 1-skeleton: since \mathcal{D} is a non-bipartite map of type $\{5, 3\}$, with Petrie polygons of length 10, such an operation must produce a non-bipartite regular $(A_5 \times C_2)$ -map of type $\{10, 3\}$, with Petrie polygons of length 5; by inspection of Table 5 and by the preceding remarks, it must be PD^0 . It follows that PD^0 is covered by the map $\{10, 3\}_5$ in Table 8 of [10], and since they both have 120 blades we have $PD^0 \cong \{10, 3\}_5$.)

Similarly the third and fourth entries in the first row each represent two S -orbits, containing 12 non-isomorphic hypermaps; they are all non-orientable, those in the third entry having characteristic -14 , branched over the 10 vertices and 6 face-centres of PD , while those in the fourth entry have characteristic -8 and are branched over the vertices of PD .

Row 2. The second row of Table 5 consists of double coverings of $\mathcal{A}_2 = PGD$ and their associates, the only significant difference from the first row being that PGD is self-dual (that is, $PGD^{(02)} \cong PGD$), so there are isomorphisms which reduce the number of hypermaps in this row from 42 to 21.

The first entry represents the great dodecahedron $\mathcal{A}_2^+ = (PGD)^+ = GD$, described in §3 and illustrated in Figure 3.4, together with its two other associates, giving three orientable hypermaps of genus 4.

As in the case of \mathcal{A}_1 , the second entry represents two S -orbits containing 12 non-isomorphic hypermaps; these have characteristic -12 and are branched over the six face-centres of PGD . They include $\mathcal{A}_2^{\hat{0}}$ and \mathcal{A}_2^0 , bipartite and non-bipartite maps of type $\{10, 5\}$;

\mathcal{A}_2^0 , which is obtained by applying Wilson’s Petrie operation to \mathcal{I} , is isomorphic to the map $\{10, 5\}_3$ in Table 8 of [10].

Since $P\mathcal{G}\mathcal{D}, \mathcal{B}^1$ and $\mathcal{B}^{\hat{1}}$ are all self-dual, so are $P\mathcal{G}\mathcal{D}^1$ and $P\mathcal{G}\mathcal{D}^{\hat{1}}$; thus the third entry represents two S -orbits of length 3, giving 6 non-isomorphic non-orientable hypermaps of characteristic -18 , branched at the 6 vertices and 6 face-centres of $P\mathcal{G}\mathcal{D}$. The 12 hypermaps represented by the fourth entry are not new: $P\mathcal{G}\mathcal{D}$ is self-dual, while \mathcal{B}^2 and $\mathcal{B}^{\hat{2}}$ are the duals of \mathcal{B}^0 and $\mathcal{B}^{\hat{0}}$, so these hypermaps are isomorphic to those given by the second entry. Thus the second row yields $3 + 2.6 + 2.3 = 21$ hypermaps.

Rows 3–6. Similarly, the remaining rows of Table 5 give double coverings of the hypermaps $\mathcal{A}_3 = W^{-1}(P\mathcal{D}^{\hat{0}})$, $\mathcal{A}_4 = W^{-1}(P\mathcal{I}^{\hat{0}})$, $\mathcal{A}_5 = P\mathcal{A}_5^+$ and $\mathcal{A}_6 = W^{-1}(P\mathcal{G}\mathcal{D}^{\hat{0}})$ constructed in §5.3. In the cases $\mathcal{A}_3, \mathcal{A}_4$ and \mathcal{A}_5 we have $\mathcal{A}_r \cong \mathcal{A}_r^{(01)}$, so the first entry of each of rows 3, 4 and 5 represents a single S -orbit of length 3 containing the orientable hypermap $\mathcal{A}_r^+ = W^{-1}(\mathcal{D}^0), W^{-1}(\mathcal{I}^0)$ and $W^{-1}(\mathcal{M}_5)$. The second entry represents two S -orbits of length 6, consisting of non-orientable hypermaps branched over the hyperedges and hyperfaces of \mathcal{A}_r . Since $\mathcal{B}^1 = (\mathcal{B}^0)^{(01)}$ and $\mathcal{B}^{\hat{1}} = (\mathcal{B}^{\hat{0}})^{(01)}$, the third entry of these three rows represents the same hypermaps as the second entry; since $\mathcal{B}^2 = (\mathcal{B}^2)^{(01)}$ and $\mathcal{B}^{\hat{2}} = (\mathcal{B}^{\hat{2}})^{(01)}$, the fourth entry represents two S -orbits of three non-orientable hypermaps, branched over the hypervertices and hyperfaces of \mathcal{A}_r .

Now $\mathcal{A}_6 = W^{-1}(P\mathcal{G}\mathcal{D}^{\hat{0}})$ is S -invariant, so the first entry in the final row represents a single S -invariant orientable hypermap $\mathcal{A}_6^+ = W^{-1}(\mathcal{G}\mathcal{D}^{\hat{0}})$. The second entry represents two S -orbits of length 3: these are non-orientable hypermaps of characteristic -36 , branched over the 6 hyperedges and 6 hyperfaces of \mathcal{A}_6 . By the S -invariance of \mathcal{A}_6 , these 6 hypermaps reappear in the third and fourth entries, so this row yields only $1 + 2.3 = 7$ hypermaps.

This gives a total of 133 hypermaps, of which 19 (namely $\mathcal{A}_1^+, \dots, \mathcal{A}_6^+$ and their associates) are orientable. Among these 133 hypermaps there are 21 maps, of which 3 (namely \mathcal{D}, \mathcal{I} and $\mathcal{G}\mathcal{D}$) are orientable. These maps, which are all obtained by applying the seven double coverings in [4] to $P\mathcal{D}, P\mathcal{I}$ and $P\mathcal{G}\mathcal{D}$, are listed and described in Table 6.

	\mathcal{A}_1^+	$\mathcal{A}_1^{\hat{0}}$	\mathcal{A}_1^0	$\mathcal{A}_1^{\hat{1}}$	\mathcal{A}_1^1	$\mathcal{A}_1^{\hat{2}}$	\mathcal{A}_1^2	\mathcal{A}_2^+	$\mathcal{A}_2^{\hat{0}}$	\mathcal{A}_2^0	$\mathcal{A}_2^{\hat{1}}$	\mathcal{A}_2^1
σ	2	2	2	2	2	2	2	1	2	2	1	1
maps in the same S -orbit	\mathcal{D} (3 2 5)	$P\mathcal{D}^{\hat{0}}$ (3 2 10)	$P\mathcal{D}^0$ (3 2 10)	$P\mathcal{D}^{\hat{1}}$ (6 2 10)	$P\mathcal{D}^1$ (6 2 10)	$P\mathcal{D}^{\hat{2}}$ (6 2 5)	$P\mathcal{D}^2$ (6 2 5)	$\mathcal{G}\mathcal{D}$ (5 2 5)	$P\mathcal{G}\mathcal{D}^{\hat{0}}$ (5 2 10)	$P\mathcal{G}\mathcal{D}^0$ (5 2 10)	$P\mathcal{G}\mathcal{D}^{\hat{1}}$ (10 2 10)	$P\mathcal{G}\mathcal{D}^1$ (10 2 10)
χ	2	-4	-4	-14	-14	-8	-8	-6	-12	-12	-18	-18
orient.	+	-	-	-	-	-	-	-	-	-	-	-
g	0	6	6	16	16	10	10	4	14	14	20	20

Table 6. The 21 regular maps \mathcal{M} with $\text{Aut } \mathcal{M} \cong A_5 \times C_2$

6.4. Two triacontahedra

In the next section we will describe how the Walsh maps of suitable associates of $\mathcal{A}_1^+, \dots, \mathcal{A}_6^+$ may be obtained from just two polyhedra, namely the *rhombic triacontahedron* \mathcal{RT} [8, §2.7] and the *small stellated triacontahedron* \mathcal{ST} [8, §6.4], so that in a sense, \mathcal{RT} and \mathcal{ST} generate all 19 of the orientable hypermaps in the previous section. For us, the most important properties of these triacontahedra are that they are bipartite maps, with $12 + 20$ and $12 + 12$ vertices respectively, and that they have automorphism groups containing $A_5 \times C_2$. This section is devoted to their construction and description.

To construct the rhombic triacontahedron \mathcal{RT} we take a dual pair \mathcal{D} and \mathcal{I} (as convex polyhedra), with their relative sizes and positions in \mathbf{R}^3 chosen so that corresponding edges of \mathcal{D} and \mathcal{I} bisect each other at right-angles. Then \mathcal{RT} is the convex hull of $\mathcal{D} \cup \mathcal{I}$ in \mathbf{R}^3 , having 30 rhombic faces (with these pairs of edges as diagonals) and 60 edges, both sets permuted transitively by

$$\text{Aut } \mathcal{RT} = \text{Aut } \mathcal{I} = \text{Aut } \mathcal{D} \cong A_5 \times C_2.$$

This group has two orbits on the vertices of \mathcal{RT} , namely the 12 5-valent vertices of \mathcal{I} and the 20 3-valent vertices of \mathcal{D} , coloured black and white in Figure 6.2. As a map, \mathcal{RT} is spherical and bipartite, but not regular.

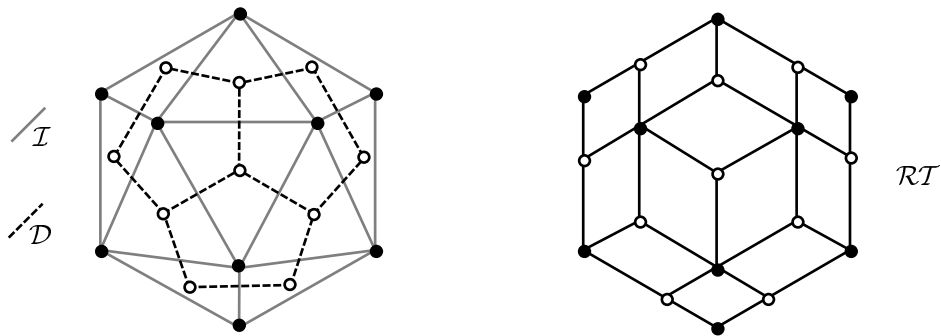


Figure 6.2. The rhombic triacontahedron \mathcal{RT}

We construct the small stellated triacontahedron \mathcal{ST} from concentric copies \mathcal{I}_- and $\mathcal{I}_+ = \lambda \mathcal{I}_-$ ($\lambda > 1$) of \mathcal{I} , the vertices v_- of \mathcal{I}_- and $v_+ = \lambda v_-$ of \mathcal{I}_+ coloured white and black respectively. Each edge vw of \mathcal{I} separates two triangular faces uvw and xvw , and we may choose λ so that the corresponding edge v_-w_- of \mathcal{I}_- and the line-segment u_+x_+ meet, bisecting each other at right-angles; then u_+, v_-, x_+ and w_- are coplanar, and are the vertices of a rhombus $u_+v_-x_+w_-$, one of the 30 such rhombic faces of \mathcal{ST} (one for each edge of \mathcal{I}_-). This is a non-convex polyhedron, with the 24 vertices of \mathcal{I}_+ and \mathcal{I}_- (the latter are hidden inside \mathcal{ST} ; in Figure 6.3, several faces are made transparent to reveal three of them).

There are 60 edges, a pair v_+w_- and v_-w_+ corresponding to each edge vw of \mathcal{I} ; in particular \mathcal{ST} is bipartite, its 1-skeleton being isomorphic to that of \mathcal{I}^0 . As a map, \mathcal{ST} has type $\{4, 5\}$ and characteristic $24 - 60 + 30 = -6$; being orientable, it has genus 4. By radial projection it is a 3-sheeted covering of the sphere, with branch-points of order 1 at the 12 vertices v_- of \mathcal{I}_- (where the vertex-figure is a pentagram $\{5/2\}$, resembling that for a vertex of \mathcal{GD}).

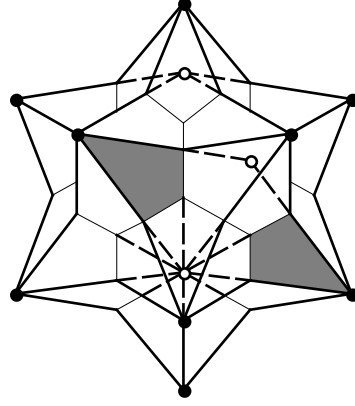


Figure 6.3. The small stellated triacontahedron \mathcal{ST} , with one face shaded and three inner vertices revealed

The Euclidean isometry group of \mathcal{ST} is equal to

$$\text{Aut } \mathcal{I}_- = \text{Aut } \mathcal{I}_+ \cong A_5 \times C_2,$$

acting transitively on its white vertices, black vertices, edges and faces. However, as a map \mathcal{ST} has the larger automorphism group

$$\text{Aut } \mathcal{ST} \cong S_5 \times C_2,$$

and is therefore regular: it is, in fact, the map $\{4, 5\}_6$, the dual of the regular map $\{5, 4\}_6$ in [10, Table 8] and [12, Tabelle II]. To see this, one checks that a cyclic permutation $(u_+v_-x_+w_-)$ of vertices around one face extends to an automorphism of order 4 interchanging black and white vertices; thus $\text{Aut}^+ \mathcal{ST}$ has order 120, contains the Euclidean rotation group isomorphic to A_5 , and has an element of order 4, so it must be isomorphic to S_5 , with the antipodal symmetry generating the factor C_2 . (Note that the “obvious” involution, transposing pairs v_+, v_- , is not an automorphism.)

6.5. Alternative constructions

We will now use the triacontahedra \mathcal{RT} and \mathcal{ST} to construct Walsh maps for representatives of each of the 6 S -orbits of regular orientable $(A_5 \times C_2)$ -hypermaps (and hence, indirectly, to obtain all 152 of the hypermaps in Tables 4 and 5).

Firstly \mathcal{ST} , being bipartite, is the Walsh map $W(\mathcal{H})$ for a hypermap \mathcal{H} ; by inspection of \mathcal{ST} , \mathcal{H} is orientable, of genus 4 and type $(5, 5, 2)$, with 12 hypervertices, 12 hyperedges and 30 hyperfaces corresponding to the black vertices, white vertices and faces of \mathcal{ST} . The isometry group of \mathcal{ST} acts as a group of automorphisms of \mathcal{H} , permuting the blades transitively, so \mathcal{H} is regular with $\text{Aut } \mathcal{H} \cong A_5 \times C_2$. We have classified all such hypermaps \mathcal{H} , and by inspection of Table 5 in §6.2 we see that \mathcal{H} must be the associate $(\mathcal{A}_2^+)^{(12)} = \mathcal{GD}^{(12)}$ of the orientable hypermap $\mathcal{A}_2^+ = \mathcal{GD}$ in the second row.

If we retain the 1-skeleton of \mathcal{ST} , but replace its rhombic faces with 20 hexagons $(u_+v_-w_+u_-v_+w_-)$, one covering each face (uvw) of \mathcal{I} as in Figure 6.4, we obtain $\mathcal{I}^{\hat{0}}$.

As we saw in §6.3, this is the Walsh map $W(\mathcal{A}_4^+)$ for the regular orientable hypermap \mathcal{A}_4^+ of type $(5, 5, 3)$, a double covering of the sphere with branch-points of order 1 at the 20 face-centres of \mathcal{I} .

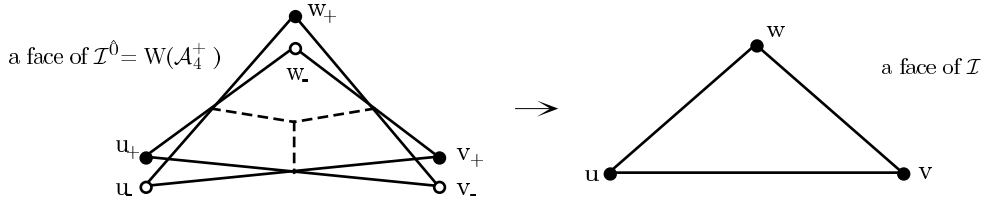


Figure 6.4. A face of $\mathcal{I}^{\hat{0}}$ covering a face of \mathcal{I}

As explained in §5.3, the map $\mathcal{M}_5 = W(\mathcal{A}_5^+)$ can be constructed from the 1-skeleton of $\mathcal{I}^{\hat{0}}$ (or equivalently of \mathcal{ST}) by attaching 20 hexagonal faces as in Figure 5.7; in this case we have a 4-sheeted covering of the sphere, with branch-points of order 2 at the 12 white vertices. Similarly, if we replace the faces of \mathcal{ST} with 12 decagons, each covering 10 faces of \mathcal{I} as in Figure 6.5, we obtain $W(\mathcal{A}_6^+)$ as a 6-sheeted covering of the sphere with branch-points of order 3 at the 12 white vertices.

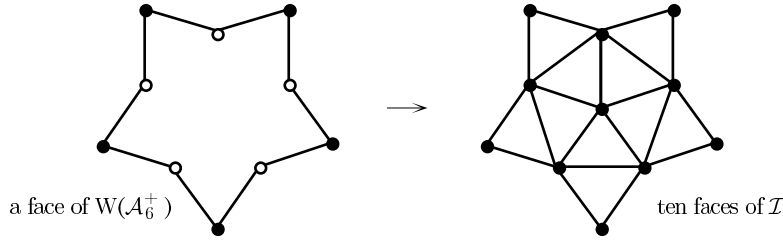


Figure 6.5. A face of $W(\mathcal{A}_6^+)$ covering 10 faces of \mathcal{I}

Representatives of the remaining S -orbits (and of at least one of those considered above) can similarly be obtained from the rhombic triacontahedron \mathcal{RT} . For example, \mathcal{RT} is the Walsh map $W(\mathcal{I}^{(12)})$ of the hypermap $\mathcal{I}^{(12)}$ of type $(5, 3, 2)$, an associate of \mathcal{I} and of $\mathcal{D} = \mathcal{A}_1^+$. If we retain the 1-skeleton of \mathcal{RT} and replace its faces with 20 hexagons, corresponding to triples of faces \mathcal{RT} around a common white vertex as in Figure 6.6, we obtain $W((\mathcal{A}_3^+)^{(02)})$, where $(\mathcal{A}_3^+)^{(02)}$, of type $(5, 3, 3)$, is the dual of \mathcal{A}_3^+ ; this is a 2-sheeted covering of the sphere with branch-points of order 1 at the 12 black vertices of \mathcal{RT} .

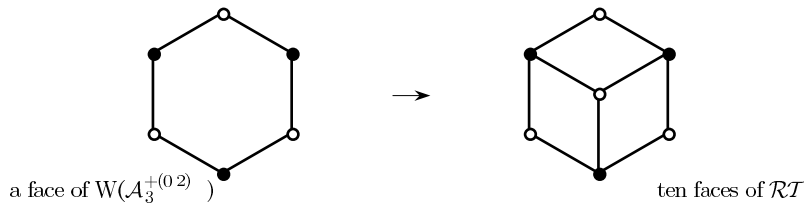


Figure 6.6. A face of $W((\mathcal{A}_3^+)^{(02)})$ covering 3 faces of \mathcal{RT}

If, instead, we replace the faces of \mathcal{RT} with 12 decagons, corresponding to quintuples of faces of \mathcal{RT} around a common black vertex as in Figure 6.7, we obtain $W((\mathcal{A}_4^+)^{(12)})$ as a double covering of the sphere with branch-points of order 1 at the 20 white vertices of \mathcal{RT} ; here $(\mathcal{A}_4^+)^{(12)}$ has type $(5, 3, 5)$.

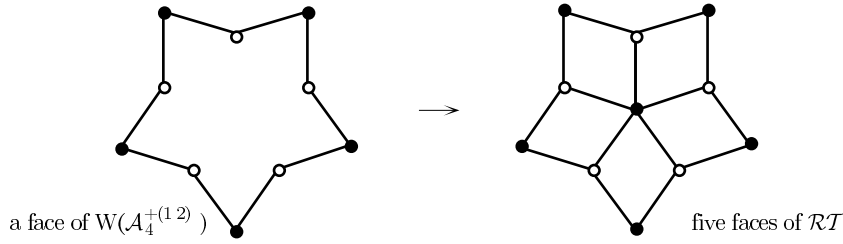


Figure 6.7. A face of $W(\mathcal{A}_4^+(12))$ covering 5 faces of \mathcal{RT}

This S -orbit, arising from both \mathcal{ST} and \mathcal{RT} , thus provides a link between these two triacontahedra.

We have now accounted for all six S -orbits of regular orientable $(A_5 \times C_2)$ -hypermaps. By taking antipodal quotients, and applying the above face-transformations to the non-orientable maps $PST = \mathcal{ST}/C_2$ and $PRT = \mathcal{RT}/C_2$, we likewise obtain the Walsh maps for representatives of the S -orbits of regular A_5 -hypermaps in §5. Since the remaining (non-orientable) regular $(A_5 \times C_2)$ -hypermaps can all be obtained from the regular A_5 -hypermaps by taking double coverings, we have shown how all the $19 + 133 = 152$ regular hypermaps in §§5–6 can be derived from \mathcal{ST} and \mathcal{RT} .

7. Regular hypermaps with automorphism group $S_4 \times C_2$

7.1. Enumeration of the hypermaps

The arguments for $G = S_4 \times C_2$ are similar to those in §§6.1–6.3 for $A_5 \times C_2$, but with two extra complications:

- 1) Unlike A_5 , S_4 has a subgroup of index 2, namely A_4 , so there exist orientable, as well as non-orientable regular S_4 -hypermaps \mathcal{S} . A further consequence is that each \mathcal{S} covers one of the seven 2-blade hypermaps \mathcal{B} (namely \mathcal{S}/A_4), so we can form only six, rather than seven disjoint products $\mathcal{H} = \mathcal{S} \times \mathcal{B}$ from \mathcal{S} .
- 2) A second complication arises from the fact that the direct decomposition of G as $S_4 \times C_2$ is not unique: although the factor C_2 , being the centre of G , is unique, there are two subgroups $S', S'' \cong S_4$, of index 2 in G , with $G = S' \times C_2 = S'' \times C_2$. (One can take G to be the isometry group of a cube, with $S' = S_4 \times \{1\}$ its rotation group and $S'' = (A_4 \times \{1\}) \cup ((S_4 \setminus A_4) \times \{-1\})$ the subgroup leaving invariant the two inscribed tetrahedra, shown in Figure 7.1.)

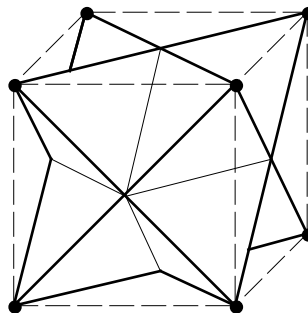


Figure 7.1. Two tetrahedra inscribed in a cube, forming a stella octangula

It follows that for each regular S_4 -hypermap \mathcal{S} , the six 2-blade hypermaps \mathcal{B} disjoint from \mathcal{S} are grouped into pairs $\mathcal{B}', \mathcal{B}''$ satisfying $\mathcal{S} \times \mathcal{B}' \cong \mathcal{S} \times \mathcal{B}''$. Since there are 13 such hypermaps \mathcal{S} (see §4.1), we therefore obtain $13 \cdot \frac{1}{2} \cdot 6 = 39$ non-isomorphic regular hypermaps $\mathcal{H} = \mathcal{S} \times \mathcal{B}$ with $\text{Aut } \mathcal{H} \cong S_4 \times C_2$. The pairing is determined by the rule that, if $\overline{\mathcal{S}}$ denotes the unique 2-blade hypermap \mathcal{S}/A_4 covered by \mathcal{S} , then $\mathcal{S} \times \mathcal{B}' \cong \mathcal{S} \times \mathcal{B}''$ if and only if $\overline{\mathcal{S}} \times \mathcal{B}' \cong \overline{\mathcal{S}} \times \mathcal{B}''$; all such isomorphisms between products of pairs of 2-blade hypermaps can be read off from Figure 8 of [4].

7.2. Description of the hypermaps

The hypermaps $\mathcal{S} = \mathcal{S}_1$ and \mathcal{S}_2 in §4 (namely \mathcal{T} and $W^{-1}(\mathcal{T}^{\hat{0}})$) are both orientable, that is, $r_0, r_1, r_2 \in S_4 \setminus A_4$, so $\overline{\mathcal{S}} = \mathcal{B}^+$; thus there is no double covering $\mathcal{H} = \mathcal{S}^+ = \mathcal{S} \times \mathcal{B}^+$, and since $\mathcal{B}^+ \times \mathcal{B}^i \cong \mathcal{B}^+ \times \mathcal{B}^{\hat{i}}$ for each i the pairing of the other six double coverings of \mathcal{S} is given by

$$\mathcal{S}^i = \mathcal{S} \times \mathcal{B}^i \cong \mathcal{S} \times \mathcal{B}^{\hat{i}} = \mathcal{S}^{\hat{i}} \quad (i = 0, 1, 2).$$

In the cases $\mathcal{S} = \mathcal{S}_3$ and \mathcal{S}_4 , we have $r_0, r_1 \in S_4 \setminus A_4$ and $r_2 \in A_4$, so $\overline{\mathcal{S}} = \mathcal{B}^2$; hence $\mathcal{S}^2 = \mathcal{S} \times \mathcal{B}^2$ does not exist, and by [4, Fig. 8] the pairing is

$$\mathcal{S}^0 \cong \mathcal{S}^1, \quad \mathcal{S}^{\hat{0}} \cong \mathcal{S}^{\hat{1}}, \quad \mathcal{S}^+ \cong \mathcal{S}^{\hat{2}}.$$

Since $\mathcal{S}_1, \dots, \mathcal{S}_4$ are without boundary, so are all 39 of the hypermaps $\mathcal{H} = \mathcal{S} \times \mathcal{B}$. Since \mathcal{S}_1 and \mathcal{S}_2 , lying in S -orbits of lengths 3 and 1, are both orientable, so are the $(1+3) \cdot 3 = 12$ non-isomorphic hypermaps \mathcal{H} arising from these orbits; the rotation group $\text{Aut}^+ \mathcal{H}$, corresponding to the subgroup of $G = S_4 \times C_2$ generated by $r_0 r_1, r_1 r_2$ and $r_2 r_0$, is isomorphic to $A_4 \times C_2$ in each case. The remaining 9 hypermaps \mathcal{S} (in S -orbits of lengths 6 and 3 containing \mathcal{S}_3 and \mathcal{S}_4) are non-orientable; each gives rise to a single orientable covering $\mathcal{H} = \mathcal{S}^+$, with rotation group $\text{Aut}^+ \mathcal{H} \cong S_4$, while the other two non-isomorphic coverings \mathcal{H} of \mathcal{S} are non-orientable (since one can check that each of the three subgroups S', S'' or $A_4 \times C_2$ of index 2 in G contains at least one of the three generators r_i of G).

	\mathcal{S}_r^+	$\mathcal{S}_r^0, \mathcal{S}_r^{\hat{0}}$	$\mathcal{S}_r^1, \mathcal{S}_r^{\hat{1}}$	\mathcal{S}_r^2	$\mathcal{S}_r^{\hat{2}}$
	$N_0 N_1 N_2 \ +/- \ g$	$N_0 N_1 N_2 \ +/- \ g$	$N_0 N_1 N_2 \ +/- \ g$	$N_0 N_1 N_2 \ +/- \ g$	$N_0 N_1 N_2 \ +/- \ g$
S_1		3 2 6 + 1	6 2 6 + 3	6 2 3 + 1	6 2 3 + 1
S_2		3 6 6 + 5	6 3 6 + 5	6 6 3 + 5	6 6 3 + 5
S_3	4 2 3 + 0	4 2 6 - 4	4 2 6 - 4		4 2 3 + 0
S_4	4 4 3 + 3	4 4 6 - 10	4 4 6 - 10		4 4 3 + 3

Table 7. The 39 regular hypermaps \mathcal{H} with $\text{Aut } \mathcal{H} \cong S_4 \times C_2$

As in §6.2 one can compute the type and characteristic of each \mathcal{H} from that of \mathcal{S} . This information is given in Table 7, each entry describing a representative $\mathcal{H} = \mathcal{S}_r \times \mathcal{B}$ of an S -orbit of length σ . For space saving, some columns were grouped together; for example, the column headed by “ $S_r^0, S_r^{\hat{0}}$ ” represents two columns S_r^0 and $S_r^{\hat{0}}$, so that the second entry of each row refers to S_r^0 and the third entry refers to $S_r^{\hat{0}}$.

7.3. Construction of the hypermaps

Row 1. The first row of Table 7 gives the double coverings \mathcal{H} of the tetrahedron $\mathcal{S}_1 = \mathcal{T}$. Those three which are maps have been determined by Vince [27, §7, Fig. 5]; they are his G'_1, G'_2 and G'_3 of types $\{3, 6\}, \{6, 3\}, \{6, 6\}$ and genera 1, 1, 3 (not 0, 0, 3, an obvious misprint).

Being orientable, \mathcal{T} yields no double covering $\mathcal{H} = \mathcal{T}^+$, so the first entry in this row is blank.

The hypermap $\mathcal{S}_1^0 = \mathcal{T}^0$ in the second entry is the torus map $\{3 + 3, 3\} = \{6, 3\}_{2,0} = \{6, 3\}_4$ in the notation of [10, Ch. 8]; it is a double covering of \mathcal{T} branched over its four face-centres, as shown in Figure 7.2 (see also [27, Fig. 5(d)]), with the edge-identifications given by the vertex-labelling.

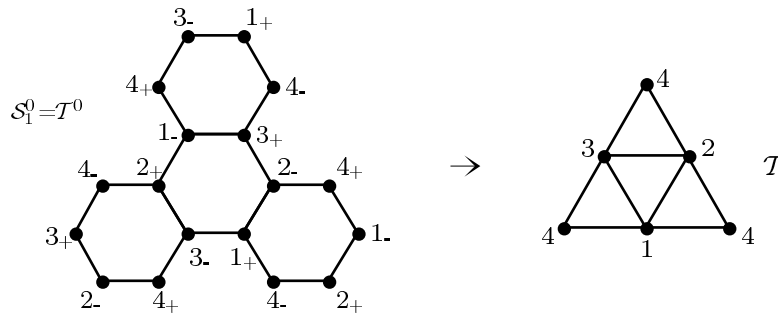


Figure 7.2. $\mathcal{S}_1^0 = \mathcal{T}^0$ as a covering of \mathcal{T}

The rotation group $\text{Aut}^+ \mathcal{T}^0$ of \mathcal{T}^0 is $A_4 \times C_2$. This map, denoted by G'_2 in [27], has five other associates, including its dual, which is Vince’s map G'_1 of type $\{3, 6\}$ and Coxeter and Moser’s $\{3, 3 + 3\} = \{3, 6\}_{2,0} = \{3, 6\}_4$. Since \mathcal{T} is orientable, \mathcal{T}^0 is isomorphic to $\mathcal{S}_1^{\hat{0}} = \mathcal{T}^{\hat{0}}$ in the third entry, and hence to the map \mathcal{W} constructed and illustrated in [4, §1].

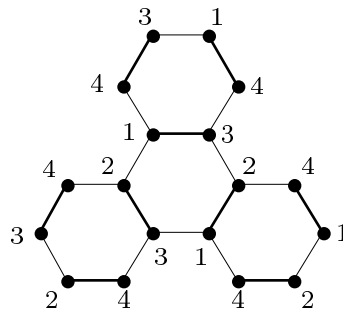


Figure 7.3. The map $\mathcal{T}^1 \cong \mathcal{T}^{\hat{1}}$

The fourth and fifth entries represent the same self-dual orientable map $\mathcal{T}^1 \cong \mathcal{T}^{\hat{1}}$ of type $\{6, 6\}$ and genus 3, branched over the vertices and face-centres of \mathcal{T} . This is Vince’s map G'_3

[27, §7, Fig. 5(e)], and Sherk’s $\{2 \cdot 3, 2 \cdot 3\}$ [23, Table V, Fig.14]. It is illustrated in Figure 7.3, where boundary edges with the same vertex-labels and the same colours are identified, so each edge of \mathcal{T} is covered by two edges of \mathcal{T}^1 . The rotation group is $A_4 \times C_2$, and there are two other associates.

Since \mathcal{T} is self-dual, the hypermap $\mathcal{T}^2 \cong \mathcal{T}^{\hat{2}}$ in the sixth and seventh entries is just the dual of $\mathcal{T}^0 \cong \mathcal{T}^{\hat{0}}$ in the second and third entries. Thus we find no further S -orbits of double coverings of \mathcal{T} , so this row yields a total of $6 + 3 = 9$ hypermaps.

Row 2. The second row of Table 7 gives the coverings \mathcal{H} of the torus hypermap $\mathcal{S}_2 = W^{-1}(\mathcal{T}^{\hat{0}})$ of type $(3, 3, 3)$ shown in Figure 4.3. As with $\mathcal{S}_1 = \mathcal{T}$, the orientability of \mathcal{S}_2 implies that there is no entry for \mathcal{S}_2^+ , and that $\mathcal{S}_2^i \cong \mathcal{S}_2^{\hat{i}}$ for $i = 0, 1$ and 2 . The orientable hypermap $\mathcal{S}_2^0 \cong \mathcal{S}_2^{\hat{0}}$ of type $(3, 6, 6)$ has genus 5, being branched over the four hyperedges and four hyperfaces of \mathcal{S}_2 . It has two other associates, and since \mathcal{S}_2 is S -invariant these three hypermaps reappear in the remaining entries in this row; they all have rotation group $A_4 \times C_2$.

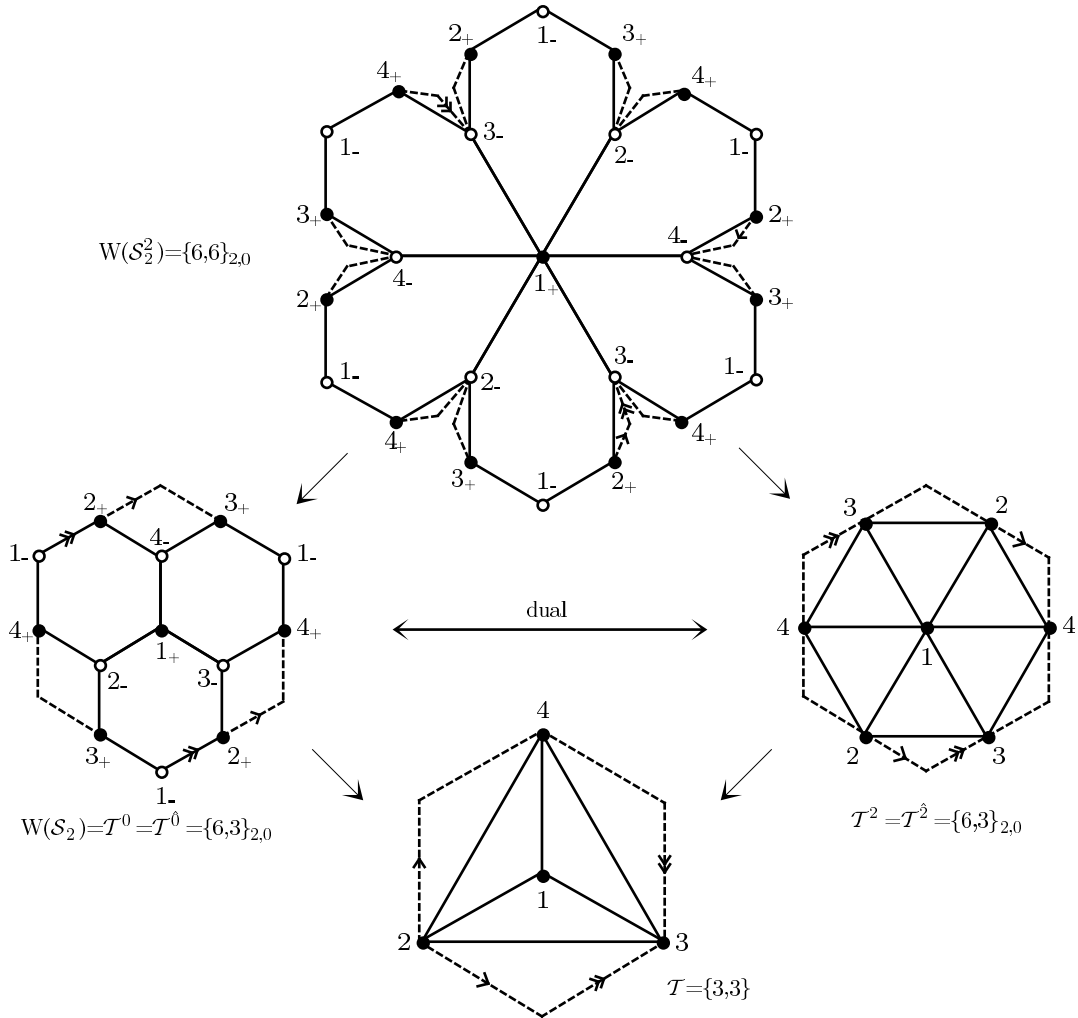


Figure 7.4. $W(\mathcal{S}_2^2) = \{6, 6\}_{2,0}$ as a double covering of the dual maps $\mathcal{T}^0 = \{6, 3\}_{2,0}$ and $\mathcal{T}^2 = \{3, 6\}_{2,0}$.

Among these, the dual hypermap $\mathcal{S}_2^2 = (\mathcal{S}_2^0)^{(02)}$, of type $(6, 6, 3)$, has Walsh map $W(\mathcal{S}_2^2)$ isomorphic to Sherk’s regular map $\{6, 6\}_{2,0}$ of genus 5 [24; 12, Tabelle III]. This is illustrated in Figure 7.4 as a double covering of the pair of dual maps $\mathcal{T}^0 = \mathcal{T}^{\hat{0}} = \{6, 3\}_{2,0}$ and $\mathcal{T}^2 = \mathcal{T}^{\hat{2}} = \{3, 6\}_{2,0}$; there are eight hexagonal faces, six around the vertex 1_+ , and two formed from the small triangles; only a few edge-identifications are shown, since the rest can be deduced by symmetry. Since \mathcal{T}^0 and \mathcal{T}^2 are double coverings of \mathcal{T} , $W(\mathcal{S}_2^2)$ is a 4-sheeted covering $\mathcal{T} \times \mathcal{B}^0 \times \mathcal{B}^2$ of \mathcal{T} , with two branch-points of order 1 over each vertex and face-centre of \mathcal{T} .

Row 3. The third row gives the double coverings of the projective octahedron $\mathcal{S}_3 = PO$, a non-orientable map of type $\{3, 4\}$ and characteristic 1 (Figure 4.4). The first entry represents its orientable double cover, the octahedron $\mathcal{O} = (PO)^+ = \{3, 4\}$, one of an S -orbit of six spherical hypermaps including its dual, the cube $\mathcal{C} = \mathcal{O}^{(02)} = \{4, 3\}$; both of these maps are illustrated in Figure 3.1.

The second and third entries in this row are a pair of non-orientable maps PO^0 and $PO^{\hat{0}}$ of type $\{6, 4\}$ and characteristic -2 , shown in Figure 7.5 (where the edge-identifications can be deduced, by symmetry about the vertex 1_+ , from those indicated); all twelve hypermaps in their two S -orbits are branched over the four face-centres of PO .

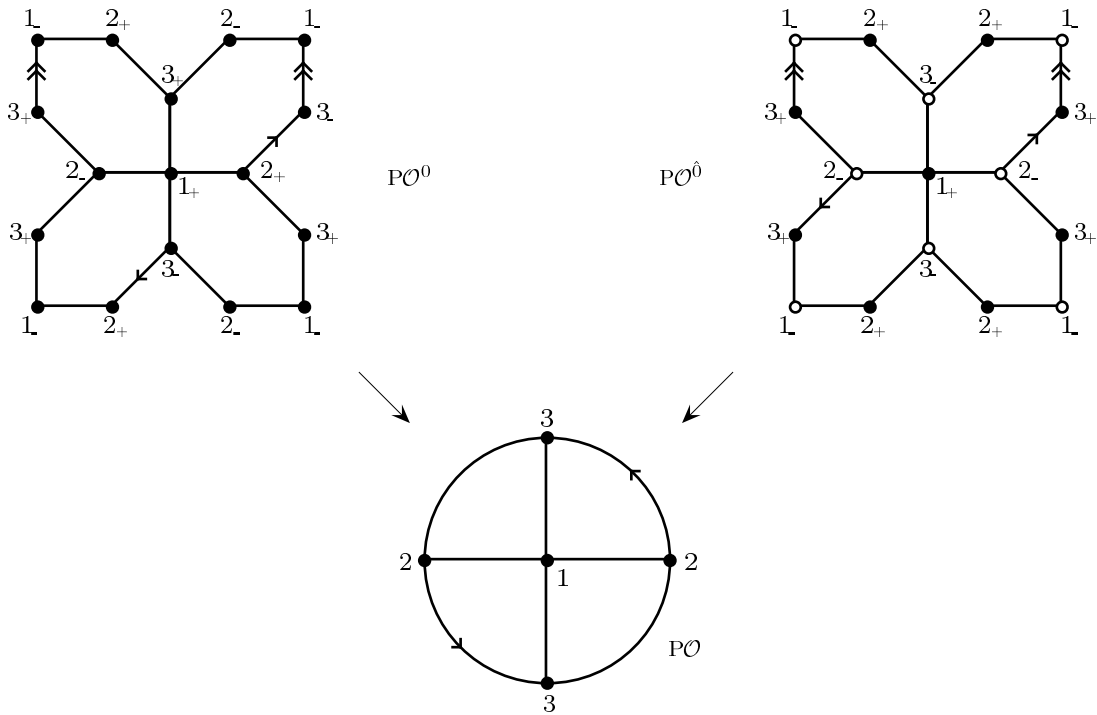


Figure 7.5. PO^0 and $PO^{\hat{0}}$ as coverings of PO

To see that $PO^0 \not\cong PO^{\hat{0}}$, note that PO^0 is bipartite, whereas $PO^{\hat{0}}$ is not (since its 1-skeleton contains circuits of odd length). Alternatively, one can demonstrate this non-isomorphism by noting that the element $g = r_0 r_1 r_2$, which has orders 3, 1 and 2 in PO, \mathcal{B}^0 and $\mathcal{B}^{\hat{0}}$, has orders 3 and 6 in PO^0 and $PO^{\hat{0}}$, so the Petrie polygons of these maps have lengths 3 and 6 respectively (see Figure 7.6).

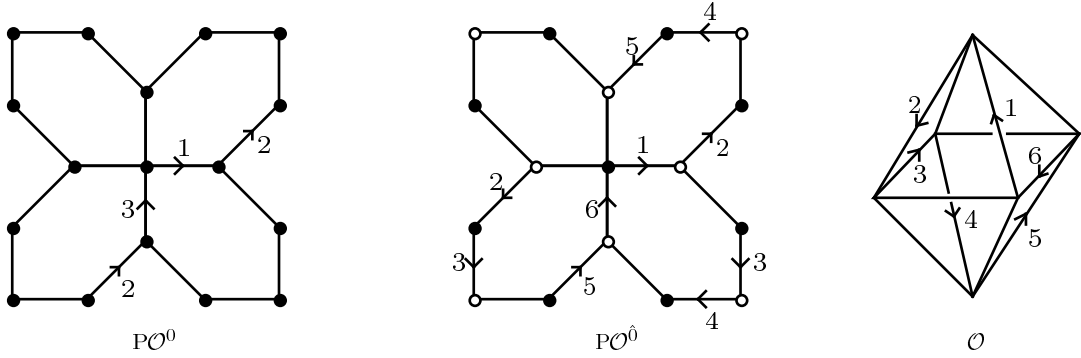


Figure 7.6. Petrie polygons in PO, PO^0 and O

It follows that PO^0 is the map $\{6, 4\}_3$ obtained by applying Wilson’s Petrie operation [29], transposing faces and Petrie polygons, to $O = \{3, 4\}_6$ (see [10, §8.6 and Table 8], and compare with the isomorphism $PD^0 \cong \{10, 3\}_5$ discussed in §6.3).

These three regular $(S_4 \times C_2)$ -hypermaps O, PO^0 and PO^0 are all quotients of the orientable map $O^0 \cong O^0$ of type $\{6, 4\}$ and genus 3 shown in Figure 7.7.

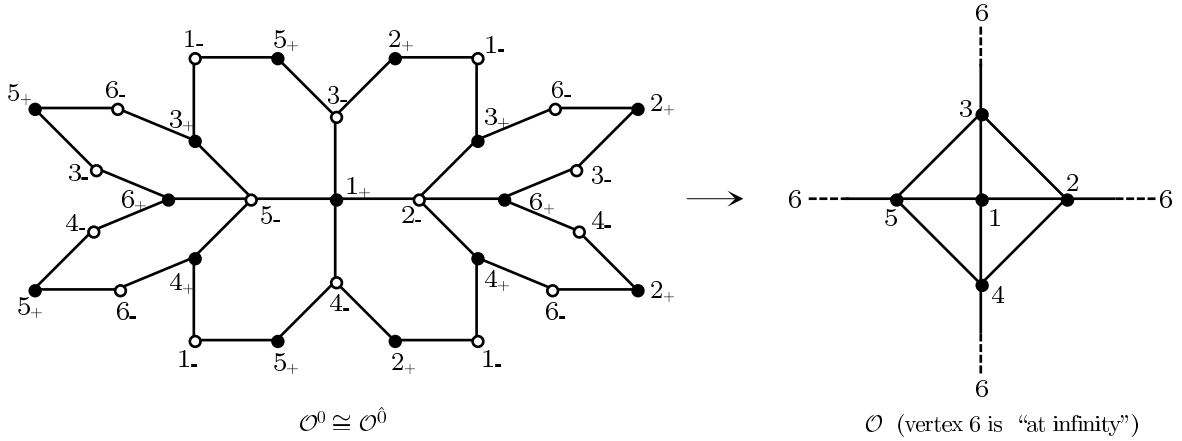


Figure 7.7. The map $O^0 \cong O^0$ as a covering of O

This map (Sherk’s $\{2 \cdot 3, 4\}$ in Table V of [23], the dual of his Figure 18) is bipartite and regular, with automorphism group

$$\text{Aut } O^0 \cong \text{Aut } O \times \text{Aut } \mathcal{B}^0 \cong S_4 \times C_2 \times C_2.$$

There are three central involutions in this group; in terms of the labelling in Figure 7.7 they are given by

$$\begin{aligned} a &: n_{\pm} \mapsto (7 - n)_{\pm}, \\ b &: n_{\pm} \mapsto n_{\mp}, \\ c &: n_{\pm} \mapsto (7 - n)_{\mp}. \end{aligned}$$

Thus a (which reverses orientation and preserves vertex-colours) is induced by the antipodal automorphism $n \mapsto 7 - n$ of O , while b (which preserves orientation and transposes vertex-colours) is the covering-transformation of $O^0 = O \times \mathcal{B}^0 \rightarrow O$ induced by the non-trivial

automorphism of $\mathcal{B}^{\hat{0}}$, and finally $c = ab = ba$. By inspection of Figures 7.7 and 7.5 it is easily seen that

$$\mathcal{O}^{\hat{0}}/\langle a \rangle \cong P\mathcal{O}^{\hat{0}}, \quad \mathcal{O}^{\hat{0}}/\langle b \rangle \cong \mathcal{O}, \quad \mathcal{O}^{\hat{0}}/\langle c \rangle \cong P\mathcal{O}^{\hat{0}}, \quad \mathcal{O}^{\hat{0}}/\langle a, b \rangle \cong P\mathcal{O}.$$

The double coverings between these maps (induced by inclusions between subgroups of $\langle a, b \rangle \cong C_2 \times C_2$) are shown in Figure 7.8.

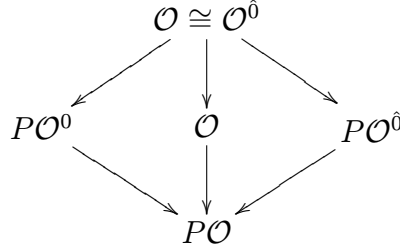


Figure 7.8. Some coverings of $P\mathcal{O}$

As explained in §7.2 we have $P\mathcal{O}^1 \cong P\mathcal{O}^0$ and $P\mathcal{O}^{\hat{1}} \cong P\mathcal{O}^{\hat{0}}$, so the associates of $P\mathcal{O}^0$ and of $P\mathcal{O}^{\hat{0}}$ also correspond to the fourth and fifth entries of this row, respectively. Since $P\mathcal{O}$ covers \mathcal{B}^2 there is no entry for $P\mathcal{O}^2$, and since $P\mathcal{O}^2 \cong P\mathcal{O}^+ \cong \mathcal{O}$ the hypermaps corresponding to the final entry are the same as those for the first, so this row contributes $6 + 6 + 6 = 18$ hypermaps.

Row 4. The final row of Table 7 gives the double coverings of the non-orientable hypermap $\mathcal{S}_4 = W^{-1}(P\mathcal{O}^{\hat{0}})$ of type $(4, 4, 3)$ and characteristic -2 shown in Figure 4.6 (see Figures 4.5 and 7.5 for $W(\mathcal{S}_4) = P\mathcal{O}^{\hat{0}}$). The first entry is the orientable double covering $\mathcal{S}_4^+ = W^{-1}(\mathcal{O}^{\hat{0}}) = W^{-1}(\mathcal{O}^0)$, of type $(4, 4, 3)$ and genus 3; its Walsh map $\mathcal{O}^{\hat{0}} = \mathcal{O}^0$ is the double covering $\{2 \cdot 3, 4\}$ of \mathcal{O} shown in Figure 7.7. This S -orbit (of length $\sigma = 3$ since the element $b \in \text{Aut } \mathcal{O}^{\hat{0}}$ induces $\mathcal{S}_4^+ \cong (\mathcal{S}_4^+)^{(01)}$) also corresponds to $\mathcal{S}_4^2 (\cong \mathcal{S}_4^+)$. The second and third entries yield two distinct S -orbits of length 3, each containing a non-orientable hypermap \mathcal{S}_4^0 or $\mathcal{S}_4^{\hat{0}}$ of type $(4, 4, 6)$ and characteristic -8 , branched over the four face-centres of \mathcal{S}_4 . As in the third row, these two S -orbits reappear in the fourth and fifth entries, while there is no entry for \mathcal{S}_4^2 . This row therefore yields $3 + 3 + 3 = 9$ hypermaps.

This gives a total of 39 hypermaps, of which 21 are orientable. Among these are 9 maps \mathcal{M} , listed in Table 8; five of these are orientable, and for these the rotation group $\text{Aut}^+ \mathcal{M}$ is indicated. As usual, χ and g denote the characteristic and genus of \mathcal{M} .

	\mathcal{S}_1^0	\mathcal{S}_1^1	\mathcal{S}_3^+	\mathcal{S}_3^0	$\mathcal{S}_3^{\hat{0}}$			
σ	2	1	2	2	2			
S -orbit	$\mathcal{T} \times \mathcal{B}^0$ (3 2 6)	$\mathcal{T} \times \mathcal{B}^2$ (6 2 3)	$\mathcal{T} \times \mathcal{B}^1$ (6 2 6)	\mathcal{O} \mathcal{C} (4 2 3) (3 2 4)	$PO \times \mathcal{B}^0$ (4 2 6)	$PC \times \mathcal{B}^2$ (6 2 4)	$PO \times \mathcal{B}^{\hat{0}}$ (4 2 6)	$PC \times \mathcal{B}^{\hat{2}}$ (6 2 4)
χ	0	-4	2	-2	-2			
orient.	+	+	+	-	-			
g	1	3	0	4	4			
$Aut^+ \mathcal{M}$	$A_4 \times C_2$	$A_4 \times C_2$	S_4	$S_4 \times C_2$	$S_4 \times C_2$			

Table 8. The 9 regular maps \mathcal{M} with $Aut \mathcal{M} \cong S_4 \times C_2$

8. Hall’s method of enumeration

In §§4–7 we needed to enumerate the normal subgroups $H \triangleleft \Delta$ with a given quotient group $\Delta/H \cong G$, or equivalently to count the orbits of $Aut G$ on generating triples $\mathbf{r} = (r_0, r_1, r_2)$ of G satisfying $r_i^2 = 1$. When G is the automorphism group $Aut \mathcal{P}$ of a Platonic solid \mathcal{P} , the comparatively simple structure of G and of $Aut G$ allows us to do this directly, by inspection, but for more complicated groups G this approach may not be feasible. Instead, one can use a technique due to P. Hall [13], which we will now describe. This has the advantage that Δ may be replaced with any finitely-generated group (see, for example, §9, where Δ^+ , a free group of rank 2, is used); the method also provides a useful numerical check in the cases where one argues by inspection.

Let Γ be any finitely-generated group, with generators X_1, \dots, X_k and defining relations $R_i(X_j) = 1$ ($i \in I$), and let G be any finite group. Our aim is to calculate

$$d_\Gamma(G) = |\mathcal{N}_\Gamma(G)|,$$

where

$$\mathcal{N}_\Gamma(G) = \{N \triangleleft \Gamma \mid \Gamma/N \cong G\}$$

(this is finite, by the assumptions on Γ and G). When Γ is understood, we will abbreviate these to $d(G)$ and $\mathcal{N}(G)$.

Each epimorphism $\varepsilon : \Gamma \rightarrow G$ gives rise to an element $N = \ker(\varepsilon)$ of $\mathcal{N}_\Gamma(G)$, and every element of $\mathcal{N}_\Gamma(G)$ arises in this way. Two epimorphisms $\varepsilon_1, \varepsilon_2 : \Gamma \rightarrow G$ have the same kernel if and only if $\varepsilon_2 = \varepsilon_1 \circ \alpha$ for some $\alpha \in Aut G$ (Figure 8.1), so $d_\Gamma(G)$ is the number of orbits of $Aut G$, acting by composition, on the set $Epi(\Gamma, G)$ of epimorphisms $\Gamma \rightarrow G$.

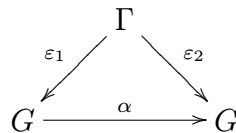


Figure 8.1. $\varepsilon_2 = \varepsilon_1 \circ \alpha$

Now we can identify $\text{Epi}(\Gamma, G)$ with the set $\mathcal{B}_\Gamma(G)$ of all Γ -bases of G : these are the k -tuples $\mathbf{x} = (x_1, \dots, x_k)$ in G such that

- (i) x_1, \dots, x_k generate G , and
- (ii) $R_i(x_j) = 1$ for all $i \in I$.

(Given ε , we define $x_j = X_j\varepsilon$, and given \mathbf{x} , we define ε by $X_j \mapsto x_j$.) Under this identification, $\text{Aut } G$ acts naturally on Γ -bases, so $d_\Gamma(G)$ is just the number of orbits of $\text{Aut } G$ on $\mathcal{B}_\Gamma(G)$. By (i), only the identity automorphism can fix any Γ -basis, so all orbits have length $|\text{Aut } G|$, and hence

$$d_\Gamma(G) = \frac{|\mathcal{B}_\Gamma(G)|}{|\text{Aut } G|} = \frac{|\text{Epi}(\Gamma, G)|}{|\text{Aut } G|}. \quad (8.1)$$

For many groups G , $|\text{Aut } G|$ is known (or is easily determined), and the main difficulty is to count epimorphisms or Γ -bases. Hall's method exploits the fact that it is generally easier to count homomorphisms $\Gamma \rightarrow G$, or equivalently k -tuples \mathbf{x} satisfying (ii) but not necessarily (i).

Let $\text{Hom}(\Gamma, G)$ denote the set of all homomorphisms $\delta : \Gamma \rightarrow G$, and define

$$\begin{aligned} \phi(G) &= \phi_\Gamma(G) = |\text{Epi}(\Gamma, G)|, \\ \sigma(G) &= \sigma_\Gamma(G) = |\text{Hom}(\Gamma, G)|. \end{aligned}$$

Each $\delta \in \text{Hom}(\Gamma, G)$ maps Γ onto a unique subgroup $H \leq G$, and conversely each epimorphism $\varepsilon : \Gamma \rightarrow H$ can be regarded as a homomorphism $\Gamma \rightarrow G$, so

$$\sigma(G) = \sum_{H \leq G} \phi(H). \quad (8.2)$$

We need to invert this equation, expressing $\phi(G) = |\text{Epi}(\Gamma, G)|$ in terms of $\sigma(G)$. Hall does this by an analogue of the Möbius Inversion Formula [14], which replaces an equation

$$f(n) = \sum_{d|n} g(d)$$

with

$$g(n) = \sum_{d|n} \mu\left(\frac{n}{d}\right) f(d),$$

where the Möbius function $\mu : \mathbf{N} \rightarrow \mathbf{Z}$ is defined by

$$\sum_{d|n} \mu(d) = \begin{cases} 1 & \text{if } n = 1, \\ 0 & \text{if } n > 1. \end{cases}$$

Let \mathcal{S} be the set of all subgroups $H \leq G$, and define the *Möbius function* $\mu = \mu_G : \mathcal{S} \rightarrow \mathbf{Z}$ recursively by

$$\sum_{H \geq K} \mu(H) = \begin{cases} 1 & \text{if } K = G, \\ 0 & \text{if } K < G. \end{cases} \quad (8.3)$$

Then (8.2) and (8.3) imply that

$$\begin{aligned}
 \sum_{H \leq G} \mu(H)\sigma(H) &= \sum_{H \leq G} \mu(H) \left(\sum_{K \leq H} \phi(K) \right) \\
 &= \sum_{K \leq G} (\phi(K) \sum_{H \geq K} \mu(H)) \\
 &= \phi(G).
 \end{aligned} \tag{8.4}$$

Substituting in (8.1), we obtain

$$d_{\Gamma}(G) = \frac{1}{|\text{Aut } G|} \sum_{H \leq G} \mu_G(H)\sigma_{\Gamma}(H). \tag{8.5}$$

If enough is known about the subgroup lattice \mathcal{S} , the values of $\mu_G(H)$ can be calculated. This can be a tedious process, though two straightforward observations ease the task:

- (a) if $H_1, H_2 \in \mathcal{S}$ are equivalent under $\text{Aut } G$, then $\sigma_G(H_1) = \sigma_G(H_2)$;
- (b) $\sigma_G(H) = 0$ unless H is an intersection of maximal subgroups of G [13, Theorem 2.3].

Hall computes $\mu_G(H)$ for several classes of groups G , including the finite rotation groups and the simple groups $PSL_2(p)$, p prime; Downs [11] has extended this to $PSL_2(q)$ for all prime-powers q .

As a simple example, take $G = A_4$. The subgroup lattice \mathcal{S} is shown in Figure 8.2: apart from A_4 and the trivial subgroup 1, \mathcal{S} contains a normal V_4 ($\cong C_2 \times C_2$), four non-normal subgroups isomorphic to C_3 , and three non-normal subgroups isomorphic to C_2 .

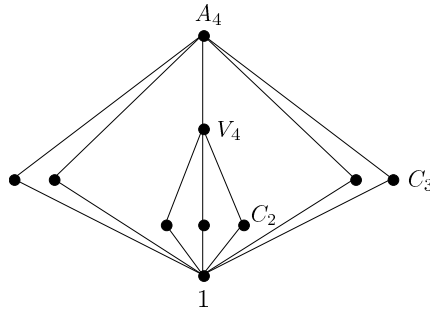


Figure 8.2. The subgroups of A_4

Applying (8.3) we find that $\mu(A_4) = 1$, $\mu(V_4) = \mu(C_3) = -1$, $\mu(C_2) = 0$ and $\mu(1) = 4$, so (8.4) takes the form

$$\phi(A_4) = \sigma(A_4) - \sigma(V_4) - 4\sigma(C_3) + 4\sigma(1). \tag{8.6}$$

Similarly, Hall obtains

$$\phi(S_4) = \sigma(S_4) - \sigma(A_4) - 3\sigma(D_4) - 4\sigma(S_3) + 3\sigma(V_4) + 4\sigma(C_3) + 12\sigma(C_2) - 12\sigma(1)$$

and

$$\phi(A_5) = \sigma(A_5) - 5\sigma(A_4) - 6\sigma(D_5) - 10\sigma(S_3) + 20\sigma(C_3) + 60\sigma(C_2) - 60\sigma(1),$$

where D_n denotes a dihedral group of order $2n$.

Once computed, the values of $\mu_G(H)$ can be used in (8.4) and (8.5) for *any* finitely-generated group Γ . The values of $\sigma_\Gamma(H)$ are most easily calculated when the defining relations $R_i(X_j) = 1$ of Γ take a simple form: thus if Γ is a free group F_k of rank k we have $\sigma_\Gamma(H) = |H|^k$, while if $\Gamma = \Delta \cong C_2 * C_2 * C_2$ we have $\sigma_\Gamma(H) = n_2(H)^3$, where $n_2(H)$ is the number of solutions of $h^2 = 1$ in H .

For example, if $G = A_4$ (so that $|\text{Aut } G| = |S_4| = 24$) then (8.5) and (8.6) give

$$d_\Delta(A_4) = \frac{1}{24}(4^3 - 4^3 - 4 \cdot 1^3 + 4 \cdot 1^3) = 0$$

(which is obvious, since A_4 cannot be generated by involutions), and

$$d_{F_2}(A_4) = \frac{1}{24}(12^2 - 4^2 - 4 \cdot 3^2 + 4 \cdot 1^2) = 4.$$

These functions d_Δ and d_{F_2} are Hall’s $c_{2,2,2}$ and d_2 ; thus his results also give $d_\Delta(S_4) = 13$ and $d_\Delta(A_5) = 19$, confirming our direct enumerations of regular S_4 - and A_5 -hypermaps in §4 and §5. Similarly $d_{F_2}(S_4) = 9$ and $d_{F_2}(A_5) = 19$, results which we will need in §9.

One can refine Hall’s method to count not only the total number of regular G -hypermaps for a given group G , but also the number of such hypermaps of any given type. For if we replace Δ with the extended triangle group $\Gamma = \Delta(l, m, n)$, obtained by adding the relations $(R_1 R_2)^l = (R_2 R_0)^m = (R_0 R_1)^n = 1$ to Δ , we find that $d_\Gamma(G)$ now gives the number of regular G -hypermaps of type (l', m', n') where l', m' and n' divide l, m and n ; by doing this for all l, m and n which arise as orders of elements of G , we obtain the required result. (Of course, for comparatively “straightforward” groups G , direct methods are more efficient, as in §§4–7.)

9. Rotary Platonic hypermaps

Let \mathcal{H} be any orientable hypermap without boundary, so its hypermap subgroup H is contained in the even subgroup Δ^+ of Δ , and its rotation group (more precisely, its orientation-preserving automorphism group) $\text{Aut}^+ \mathcal{H}$ is isomorphic to $N_{\Delta^+}(H)/H$. We call \mathcal{H} *rotary* if $\text{Aut}^+ \mathcal{H}$ acts transitively on the set of “brins” of \mathcal{H} (the cycles of r_2 on the set Ω of blades); equivalently, H is normal in Δ^+ , so $\text{Aut}^+ \mathcal{H} \cong \Delta^+/H$. (Our terminology follows Vince and Wilson, rather than Coxeter and Moser who use the terms “reflexible” and “regular” where we have used “regular” and “rotary”.) If \mathcal{H} is regular then it is rotary (since normality of H in Δ implies normality in Δ^+), but not conversely. If \mathcal{H} is rotary but not regular it is called *chiral*; such hypermaps occur in mirror-image pairs, with mutually reversed orientations, corresponding to pairs of normal subgroups H of Δ^+ which are conjugate in Δ . For example, the torus map $\{4, 4\}_{b,c}$ of [10, §8.3] is regular if $bc(b - c) = 0$, but is chiral (with mirror-image $\{4, 4\}_{c,b}$) if $bc(b - c) \neq 0$ (see Figure 9.1).

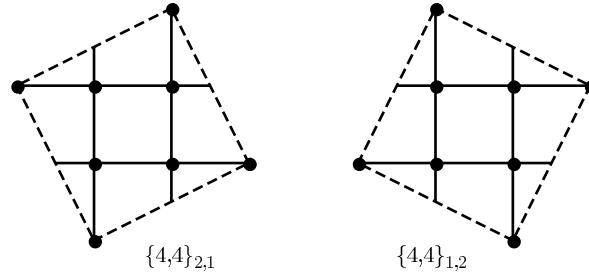


Figure 9.1. The chiral maps $\{4, 4\}_{2,1}$ and $\{4, 4\}_{1,2}$

Now suppose that \mathcal{H} is any rotary hypermap with rotation group $\text{Aut}^+\mathcal{H} \cong \text{Aut}^+\mathcal{P}$ for some Platonic solid \mathcal{P} . Then there are three possibilities:

- i) \mathcal{H} is regular, with $\text{Aut } \mathcal{H} \cong \text{Aut } \mathcal{P}$;
- ii) \mathcal{H} is regular, with $\text{Aut } \mathcal{H} \not\cong \text{Aut } \mathcal{P}$;
- iii) \mathcal{H} is not regular, that is, \mathcal{H} is chiral.

We have already determined the hypermaps \mathcal{H} satisfying i), and our aim is now to show that cases ii) and iii) do not occur.

Theorem. *If \mathcal{H} is a rotary hypermap, with $\text{Aut}^+\mathcal{H} \cong \text{Aut}^+\mathcal{P}$ for some Platonic solid \mathcal{P} , then \mathcal{H} is regular with $\text{Aut } \mathcal{H} \cong \text{Aut } \mathcal{P}$.*

To prove this, we note that for any group G , the rotary hypermaps \mathcal{H} with $\text{Aut}^+\mathcal{H} \cong G$ are in bijective correspondence with the normal subgroups H of Δ^+ with $\Delta^+/H \cong G$; since Δ^+ is a free group of rank 2 (with basis R_0R_1, R_1R_2) they correspond to the orbits of $\text{Aut } G$ on generating pairs for G .

First let \mathcal{P} be the tetrahedron \mathcal{T} , so that $G = \text{Aut}^+\mathcal{T}$ can be identified with A_4 , and $\text{Aut } G$ with S_4 acting by conjugation on G . By inspection, or by Hall’s method (as in §8) one easily finds that $d_{F_2}(G) = 4$, so that $\text{Aut } G$ has four orbits on generating pairs for G : the two generators can have orders 2 and 3, or 3 and 2, or 3 and 3, and in this last case they may or may not be conjugate in G . Thus there are, up to orientation-preserving isomorphism, four rotary hypermaps \mathcal{H} with $\text{Aut}^+\mathcal{H} \cong A_4$. We saw in §4 that among the 13 regular S_4 -hypermaps, four are orientable, with rotation group A_4 . Clearly these are rotary, so they must be the four rotary hypermaps \mathcal{H} we have just enumerated. (In fact, the four orbits on generating pairs correspond to the hypermaps $\mathcal{T}^{(12)}, \mathcal{T}^{(01)}, \mathcal{T}$ and $\mathcal{S}_2 = W^{-1}(\mathcal{T}^0)$ respectively.) Thus each of the four rotary hypermaps \mathcal{H} with $\text{Aut}^+\mathcal{H} \cong \text{Aut}^+\mathcal{T}$ is regular, with $\text{Aut } \mathcal{H} \cong S_4 \cong \text{Aut } \mathcal{T}$.

A similar method can be used in the remaining cases. When $\mathcal{P} = \mathcal{O}$ (or equivalently \mathcal{C}), we put $G = \text{Aut}^+\mathcal{O} \cong S_4$, so that $\text{Aut } G \cong S_4$, acting on itself by conjugation. Either by inspection or by Hall’s method we find that S_4 has 9 conjugacy classes of generating pairs, so there are 9 rotary hypermaps \mathcal{H} with $\text{Aut}^+\mathcal{H} \cong \text{Aut}^+\mathcal{O}$. Now in §7 we found 39 regular $(S_4 \times C_2)$ -hypermaps \mathcal{H} , 21 of them orientable; among these, 9 have $\text{Aut}^+\mathcal{H} \cong S_4$, namely the six associates of $\mathcal{S}_3^+ = \mathcal{O}$ and the three associates of $\mathcal{S}_4^+ = W^{-1}(\mathcal{O}^0)$. These must be the 9 rotary hypermaps previously enumerated, so again the result is verified.

Likewise, when $\mathcal{P} = \mathcal{D}$ or \mathcal{I} we put $G \cong A_5$, so $\text{Aut } G \cong S_5$, again acting by conjugation. By [13], $d_{F_2}(G) = 19$ so there are 19 rotary hypermaps \mathcal{H} with $\text{Aut}^+\mathcal{H} \cong G$, and these must

be the 19 regular orientable $(A_5 \times C_2)$ -hypermaps listed in Table 5 (§6.2). This completes the proof.

References

- [1] Brahana, H. R.: *Regular maps and their groups*. Amer. J. Math. **49** (1927), 268–284.
- [2] Brahana, H. R.; Coble, A. B.: *Maps of twelve countries with five sides with a group of order 120 containing an icosahedral subgroup*. Amer. J. Math. **48** (1926), 1–20.
- [3] Breda d'Azevedo, A. J.: Ph.D. thesis, University of Southampton, 1991.
- [4] Breda d'Azevedo, A. J.; Jones, G. A.: *Double coverings and reflexible abelian hypermaps*. Preprint.
- [5] Breda d'Azevedo, A. J.; Jones, G. A.: *Rotary hypermaps of genus 2*. Preprint.
- [6] Cori, R.; Machì, A.: *Maps, hypermaps and their automorphisms: a survey I, II, III*. Expositiones Math. **10** (1992), 403–427, 429–447, 449–467.
- [7] Corn, D.; Singerman, D.: *Regular hypermaps*. Europ. J. Comb. **9** (1988), 337–351.
- [8] Coxeter, H. S. M.: *Regular Polytopes*. Dover, New York, 3rd ed. 1973.
- [9] Coxeter, H. S. M.: *Geometry*. Wiley, New York/London 1961.
- [10] Coxeter, H. S. M.; Moser, W. O. I.: *Generators and Relations for Discrete Groups*. Springer-Verlag, Berlin/Heidelberg/New York, 4th ed. 1972.
- [11] Downs, M. N. L.: *The Möbius function of $PSL_2(q)$, with application to the maximal normal subgroups of the modular group*. J. London Math. Soc. **43** (1991), 61–75.
- [12] Garbe, D.: *Über die regulären Zerlegungen geschlossener orientierbarer Flächen*. J. Reine Angew. Math **237** (1969), 39–55.
- [13] Hall, P.: *The Eulerian functions of a group*. Quarterly J. Math. Oxford **7** (1936), 134–151.
- [14] Hardy, G. H.; Wright, E. M.: *Introduction to the Theory of Numbers*. Oxford University Press, Oxford 1979.
- [15] Izquierdo, M.; Singerman, D.: *Hypermaps on surfaces with boundary*. Europ. J. Comb. **15** (2) (1994), 159–172.
- [16] James, L. D.: *Operations on hypermaps, and outer automorphisms*. Europ. J. Comb. **9** (1988), 551–560.
- [17] Jones, G. A.: *Symmetry*. In: Handbook of Applicable Mathematics. Vol. 5, Combinatorics and Geometry (ed. W. Ledermann), Wiley, Chichester/New York/London 1985, 329–422.
- [18] Jones, G. A.: *Ree groups and Riemann surfaces*. J. Algebra **165** (1) (1994), 41–62.

- [19] Jones, G. A.; Silver, S. A.: *Suzuki groups and surfaces*. J. London Math. Soc. (2) **48** (1993), 117–125.
- [20] Jones, G. A.; Thornton, J. S.: *Operations on maps, and outer automorphisms*. J. Combinatorial Theory, Ser. B, **35** (1983), 93–103.
- [21] Machì, A.: *On the complexity of a hypermap*. Discr. Math. **42** (1982), 221–226.
- [22] Robertson, S. A.: *Polytopes and Symmetry*. London Math. Soc. Lecture Note Series **90**, Cambridge University Press, Cambridge 1984.
- [23] Sherk, F. A.: *The regular maps on a surface of genus three*. Canadian J. Math. **11** (1959), 452–480.
- [24] Sherk, F. A.: *A family of regular maps of type $\{6, 6\}$* . Canadian Math. Bull. **5** (1962), 13–20.
- [25] Simon, J.: *Du Commentaire de Proclus sur le Timée*. Paris 1839.
- [26] Threlfall, W.: *Gruppenbilder*. Abh. sächs. Akad. Wiss. Math.-phys. Kl., **41** (1932), 1–59.
- [27] Vince, A.: *Regular combinatorial maps*. J. Combinatorial Theory, Ser. B, **34** (1983), 256–277.
- [28] Walsh, T. R. S.: *Hypermaps versus bipartite maps*. J. Combinatorial Theory, Ser. B, **18** (1975), 155–163.
- [29] Wilson, S. E.: *Operators over regular maps*. Pacific J. Math. **81** (2) (1979), 559–568.
- [30] Wilson, S. E.: *Cantankerous maps and rotary embeddings of K_n* . J. Combinatorial Theory, Ser. B, (1989).

Received August 30, 1999